Gravity and matter on a pure geometric thick polynomial $f(R)$ brane

Heng Guo[*]

School of Physics, Xidian University, Xi'an 710071, China

Lang-Lang Wang[†]

*School of Physics, Xidian University, Xi'an 710071, China and School of General Education,
Shanxi Institute of Science and Technology, Jincheng 048000, China*

Chun-E Fu[‡]

School of Science, Xi'an Jiaotong University, Xi'an 710049, China

Qun-Ying Xie[§]

School of Information Science and Engineering, Lanzhou University, Lanzhou 730000, China

In this paper, writing the most general form $f(R) = \sum_{i=1}^{n} a_i R^i + \Lambda$ the solutions of the pure geometric thick $f(R)$ brane are investigated. For the certain value of n, the analytical thick brane solution can be calculated, and when $n = 3$, $n = 4$, and $n = 10$, the thick brane solutions are presented. The solutions are stable against linear tensor perturbations. The zero mode of gravity and scalar field can be localized on thick $f(R)$ branes naturally. The zero mode of a vector field and left-chiral fermion can be localized on thick $f(R)$ branes by introducing the coupling with scalar curvature R of spacetime, and the massive resonant modes can be quasilocalized on the brane with the large coupling coefficients.

I. INTRODUCTION

The idea that our four-dimensional (4D) Universe can be considered as a brane embedded in a higher-dimensional spacetime, can supply new insights for solving the gauge hierarchy problem [1–8] and the cosmological constant problem [9–21]. In the Randall-Sundrum (RS) braneworld model [22], the effective 4D gravity could be recovered even in the case of noncompact extra dimensions, however, singularities are present at the position of the branes. The smooth thick braneworld solutions are generally based on gravity coupled to bulk scalar fields [23–62]. For some comprehensive reviews about thick branes, please see Refs. [63–67]. There are also thick branes arising from pure geometry without the inclusion of bulk scalar fields at all [68–77].

---

[*]Corresponding author.
hguo@xidian.edu.cn
[†]wllsrr@163.com
[‡]fuche13@mail.xjtu.edu.cn
[§]xieqy@lzu.edu.cn

In braneworld scenarios, the important issue is the localization of gravity and various bulk matter fields for the purpose of recovering the effective 4D gravity and building up the standard model. Generally the gravity and the scalar field zero mode can be localized on the brane naturally. For five-dimensional (5D) free spin-1 Abelian vector field, the zero mode cannot be trapped on the Minkowski ($\mathcal{M}_4$) brane, however, it can be localized on the thick de Sitter brane and Weyl thick brane [8,78–81]. In some ways, by introducing the coupling with background geometry, the zero mode of the vector field can also be trapped on the Minkowski brane [82,83]. For the spin-1/2 fermion, zero mode cannot be localized on the branes without introducing the coupling. By introducing the coupling between the fermion and background scalar fields or fermion and background geometry, the left-chiral fermion zero mode can be localized on the brane [8,16,48,78–80,84–129].

However, due to the fact that Einstein's general relativity is not renormalizable, the effects of higher order curvature terms are suggested to consider. $f(R)$ gravity theories, which the Lagrangians are proportional to some functions of the scalar curvature R, were created in the investigation of cosmology, and offer pure geometric explanations for cosmological inflation and dark energy in physically [130–137]. Nevertheless, there are studies devoted to embedding branes into various types of $f(R)$ gravities [6,41,50,57–60,73,74,77,138–150]. In Ref. [77],

two cases of the thick brane solutions have been investigated in pure geometry $f(R)$ gravities: one with a triangular $f(R)$ and the other a simple polynomial $f(R)$.

In this paper, we intend to investigate the thick branes generated by only geometry under pure $f(R)$ gravity. The general form of $f(R)$ would be considered, which is chosen as a nth order polynomial of the scalar curvature R. When the degree of the polynomial $f(R)$ is $n = 3$, the solution is equivalent to the one of Ref. [77], When $n = 4$ and $n = 10$, the solutions are new solutions. These solutions will be presented in next section. The stability of tensor perturbations and the localization of gravity are discussed in Sec. III. The zero mode of gravity can be localized on the brane naturally. In Sec. IV, the zero mode of the scalar field can be trapped on the branes naturally. In Sec. V, by introducing the coupling between the vector field and the background geometry, the zero mode vector can be localized on the brane and the massive resonant Kaluza-Klein (KK) modes can also be quasilocalized on the brane. In Sec. VI, for a pure geometry brane, the coupling between the fermion and the background scalars cannot be introduced, however, we introduce the coupling between the fermion and the background geometry, and the zero mode of the left-chiral fermion and the massive resonant KK modes can be localized and quasilocalized on the brane. Finally, the conclusion and discussion are given in Sec. VII.

II. THE PURE GEOMETRIC THICK $f(R)$ BRANES

We start with the following 5D action for a pure geometric thick $f(R)$ braneworld

$$S = \frac{1}{2\kappa_5^2} \int d^5x \sqrt{-g} f(R), \tag{1}$$

where $\kappa_5^2 = 8\pi G_5$ with G_5 being the 5D Newton constant, R is the 5D scalar curvature, and $g = \det(g_{MN})$ is the determinant of the metric. Throughout this paper, capital Latin letters $M, N, \cdots = 0, 1, 2, 3, 5$ and Greek letters $\mu, \nu, \cdots = 0, 1, 2, 3$ are used to represent the bulk and brane indices, respectively. From this action, the 5D Einstein equation is given by

$$R_{MN} f_R - \frac{1}{2} g_{MN} f(R) + (g_{MN}\Box - \nabla_M \nabla_N) f_R = 0, \tag{2}$$

where $f_R \equiv \frac{df(R)}{dR}$, $\Box = g^{MN}\nabla_M\nabla_N$ is the 5D d'Alembert operator, and R_{MN} is the 5D Ricci tensor, defined in terms of the Riemann tensor $R_{MN} = R^Q_{MQN}$.

The line element of the $\mathcal{M}_4$ brane is assumed as

$$ds^2 = g_{MN} dx^M dx^N = e^{2A(y)} \eta_{\mu\nu} dx^\mu dx^\nu + dy^2, \tag{3}$$

where $e^{2A(y)}$ is the warp factor,

$$\eta_{\mu\nu} = \text{diag}(-1, +1, +1, +1) \tag{4}$$

is the metric of the 4D Minkowski spacetime, and y denotes the extra dimensional coordinate. From the metric (3), the Ricci tensor and scalar curvature can be computed:

$$R_{\mu\nu} = -e^{2A(y)}(A'' + 4A'^2)\eta_{\mu\nu}, \quad R_{55} = -4A'' - 4A'^2, \tag{5}$$

$$R = -20A'^2 - 8A'', \tag{6}$$

where the prime denotes the derivatives with respect to extra dimensional coordinate y. The Einstein equations (2) can be rewritten as:

$$f(R) + 2f_R(4A'^2 + A'') - 6f'_R A' - 2f''_R = 0, \tag{7a}$$

$$-f(R) - 8f_R(A'' + A'^2) + 8f_R A' = 0. \tag{7b}$$

The above two equations are not independent, because the left side of Eq. (2) is divergence free [134]. Hence, we choose to solve Eq. (7a) in the following discussion.

In this paper, we are interested in investigating the general form of $f(R)$, chosen as a nth order polynomial of the scalar curvature R:

$$f(R) = \sum_{i=1}^{n} a_i R^i + \Lambda, \tag{8}$$

where the a_i coefficients have the appropriate dimensions, Λ is 5D cosmological constants, and the parameter n should be an integer.

According to Eqs. (6) and (8), one can easily prove that $f(R)$ includes $(A'')^n$ and $(A')^{2n}$, f'_R includes A''' and f''_R includes A''''. By taking $f(R)$, f'_R, and f''_R back into Eq. (7), obviously, the Einstein equations are high-order differential equations, and very hard to be solved. In order to find a solution, we begin with a simple $A(y)$, which consider as [77,150]

$$A(y) = -\delta \ln(\cosh(ky)) \tag{9}$$

with δ a dimensionless positive constant, and k another positive constant with the dimension of length inverse. At the infinity, the behavior of the $A(y \to \infty)$ is

$$A(y \to \infty) \to -\delta k|y|. \tag{10}$$

Defining a new parameter by $\tilde{k} = \delta k$, it is easy to proof that the warp factor

$$e^{2A(y\to\infty)} \to e^{-2\tilde{k}|y|}, \tag{11}$$

which is the same as the warp fact of the RS II braneworld and implies that the metric (3) reduces an anti–de

Sitter (AdS) one, which is essential for the localization of gravitation. The following expressions can also be taken

$$A'(y) = -\delta k \tanh(ky), \tag{12}$$

$$A'^2(y) = \delta^2 k^2 (1 - \text{sech}^2(ky)), \tag{13}$$

$$A''(y) = -\delta k^2 \text{sech}^2(ky), \tag{14}$$

and the scalar curvature takes a simple form:

$$R(y) = 20\delta^2 k^2 (\varepsilon \text{sech}^2(ky) - 1), \tag{15}$$

where $\varepsilon = \frac{5\delta + 2}{5\delta}$. Furthermore, we can obtain the following expressions

$$f(R) = \sum_{i=1}^{n} a_i (20\delta^2 k^2)^i (\varepsilon \text{sech}^2(ky) - 1)^i + \Lambda, \tag{16}$$

$$f_R = \sum_{i=1}^{n} i \, a_i (20\delta^2 k^2)^{i-1} (\varepsilon \text{sech}^2(ky) - 1)^{i-1}, \tag{17}$$

$$f'_R = \sum_{i=1}^{n} 2i(1-i) a_i k \varepsilon (20\delta^2 k^2)^{i-1} \text{sech}^2(ky) \tanh(ky)$$
$$\times (\varepsilon \text{sech}^2(ky) - 1)^{i-2}, \tag{18}$$

$$f'_R A' = \sum_{i=1}^{n} 2i(i-1) a_i \delta k^{2i} \varepsilon (20\delta^2)^{i-1} \text{sech}^2(ky)$$
$$\times (1 - \text{sech}^2(ky))(\varepsilon \text{sech}^2(ky) - 1)^{i-2}, \tag{19}$$

$$f''_R = \sum_{i=1}^{n} 2i(i-1) a_i \varepsilon k^{2i} (20\delta^2)^{i-1} (\varepsilon \text{sech}^2(ky) - 1)^{i-3}$$
$$\times \text{sech}^2(ky) [2(i-2)\varepsilon \text{sech}^2(ky)(1 - \text{sech}^2(ky))$$
$$+ (2 - 3\text{sech}^2(ky))(\varepsilon \text{sech}^2(ky) - 1)] \tag{20}$$

By taking above expressions back into Eq. (7a), it is clear that all the terms of the Einstein equation are the function of $\text{sech}^2(ky)$, and the order of the highest is $2n$. The Einstein equation (7a) can be expressed as the following algebraic equation:

$$\sum_{i=0}^{n} B_i \text{sech}^{2i}(ky) = 0, \tag{21}$$

where the coefficient B_i can be written as follows

$$B_i = \sum_{j=i}^{n} (-1)^{j-i} 2a_j (20\delta^2)^{j-1} k^{2j} \varepsilon^{i-1}$$
$$\times [10\delta^2 C_j^i \varepsilon - j\delta(4\delta C_{j-1}^i \varepsilon + (1 + 4\delta) C_{j-1}^{i-1})$$
$$+ 2j(j-1)((2 + 3\delta) C_{j-2}^{i-1} \varepsilon + (3 + 3\delta) C_{j-2}^{i-2})$$
$$+ 4j(j-1)(j-2)(C_{j-3}^{i-2} \varepsilon + C_{j-3}^{i-3})], \tag{22}$$

with $a_0 \equiv \Lambda$ and C_j^i the binomial coefficient. Here we define $C_j^i \equiv 0$ when $i > j$. The B_i can also be expressed as a column matrix:

$$\begin{pmatrix} B_0 \\ B_1 \\ \vdots \\ B_{n-1} \\ B_n \end{pmatrix} = \begin{pmatrix} b_{0,0} & b_{0,1} & \cdots & b_{0,n-1} & b_{0,n} \\ b_{1,0} & b_{1,1} & \cdots & b_{1,n-1} & b_{1,n} \\ \vdots & \vdots & b_{i,j} & \vdots & \vdots \\ b_{n-1,0} & b_{n-1,1} & \cdots & b_{n-1,n-1} & b_{n-1,n} \\ b_{n,0} & b_{n,1} & \cdots & b_{n,n-1} & b_{n,n} \end{pmatrix}_{((n+1)\times(n+1))} \begin{pmatrix} a_0 \\ a_1 \\ \vdots \\ a_{n-1} \\ a_n \end{pmatrix}, \tag{23}$$

where the element of the matrix $b_{i,j}$ is

$$b_{i,j} = (-1)^{j-i} 2(20\delta^2)^{j-1} k^{2j} \varepsilon^{i-1}$$
$$\times [10\delta^2 C_j^i \varepsilon - j\delta(4\delta C_{j-1}^i \varepsilon + (1 + 4\delta) C_{j-1}^{i-1})$$
$$+ 2j(j-1)((2 + 3\delta) C_{j-2}^{i-1} \varepsilon + (3 + 3\delta) C_{j-2}^{i-2})$$
$$+ 4j(j-1)(j-2)(C_{j-3}^{i-2} \varepsilon + C_{j-3}^{i-3})]. \tag{24}$$

By setting all the coefficients to zero $B_i = 0$, the solution to the Eq. (21) can be calculated. Analyzing the expression

(24), when $i > j$, it is easy to find that $b_{i,j} = 0$, since all the binomial coefficients are zero. Specially, except for $b_{n,n}$, the elements of the last row of the matrix are zero, so the coefficient B_n satisfies the following formulation

$$B_n = 2k^2 a_n (20\delta^2 k^2)^{n-1} \varepsilon^{n-1} [(10 - 4n)\delta^2$$
$$+ (6n^2 - 7n + 4)\delta + (4n^3 - 6n^2 + 2n)] = 0. \tag{25}$$

For nonzero solution of a_n, the relationship between δ and n can be calculated as follows
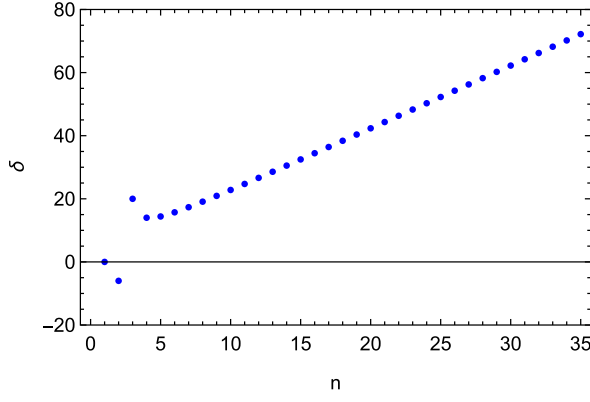
FIG. 1. The relation between the parameter δ and n.

$$\delta = \frac{4n^2 - 6n + 2}{2n - 5}. \tag{26}$$

For each certain value of n, the parameter δ can be obtained as it is depicted in Fig. 1. In order to ensure that the behavior of warp factor at infinity tends to zero, δ must be positive definite, so the minimum value of the positive integer n is $n_{\min} = 3$. It is easy to see that when $n = 4$, the minimum δ can be achieved $\delta_{\min} = 14$, and when n tends to infinity, δ is proportional to n and tends to divergence.

Furthermore, Eq. (23) can be reexpressed as follows

$$\begin{pmatrix} 1 & b_{0,1} & \cdots & b_{0,n-1} & b_{0,n} \\ 0 & b_{1,1} & \cdots & b_{1,n-1} & b_{1,n} \\ \vdots & \vdots & b_{i,j} & \vdots & \vdots \\ 0 & 0 & \cdots & b_{n-1,n-1} & b_{n-1,n} \\ 0 & 0 & \cdots & 0 & 0 \end{pmatrix}_{(n+1)\times(n+1)} \begin{pmatrix} \Lambda \\ a_1 \\ \vdots \\ a_{n-1} \\ a_n \end{pmatrix} = \begin{pmatrix} 0 \\ 0 \\ \vdots \\ 0 \\ 0 \end{pmatrix}. \tag{27}$$

By considering the Eqs. (24) and (26), all the elements of the matrix $b_{i,j}$ can be calculated for the given value of n, so the matrix equation (27) contains n linear equations and $n + 1$ unknown parameters $\Lambda, a_1, a_2, a_3, \ldots, a_n$, and the relationships of these parameters could be concluded by solving Eq. (27).

When $n = 1$ and $f(R) = a_1 R + \Lambda$, the case of general relativity is recovered. Because $\delta = 0$ and $A(y) = 0$, there is no pure geometric thick $\mathcal{M}_4$ brane solution. However, by using a different metric ansatz, a de Sitter dS_4 brane solution can be obtained, which has been studied in Refs. [8,151], or by introducing the tension of the brane, the RS braneworld model [3,22] can also be concluded.

When $n = 2$ and $f(R) = a_1 R + a_2 R^2 + \Lambda$, the parameter $\delta = -6$ and $A(y) = 6 \ln(\cosh(ky))$, thus the warp factor $e^{2A(y)} = \cosh^{12}(ky)$ is divergent at infinity of the extra dimensional coordinate. By introducing a background scalar, the divergence of warp factor is removed and the thick branes can be constructed in Ref. [50,57,147].

When $n = 3$, the parameter $\delta = 20$ and warp factor $A(y) = -20 \ln(\cosh(ky))$, and a pure geometric thick $\mathcal{M}_4$ brane can be received. When $n = 4$, the parameter δ can be achieved the minimum value $\delta = \delta_{\min} = 14$, and a pure geometric thick $\mathcal{M}_4$ brane can also be constructed. When $n = 5, 6, \ldots$, the solutions of a thick $\mathcal{M}_4$ brane can be concluded, however, as the value of the parameter n increases, the calculation also increases. In this paper, the solutions will be discussed when $n = 3$ (for the minimum n), $n = 4$ (for the minimum δ), and $n = 10$ (for a large value n), and these cases are very typical. The parameters of the solutions are shown in Table I. Here, the coefficient a_1 is set to positive, so the 5D cosmological constant must be negative $\Lambda < 0$, and the 5D spacetime is AdS one. Moreover, the coefficients a_i for the solutions are shown in Fig. 2, and it can be found that the coefficients a_i significantly decreases with increasing the order i. For the case of $n = 3$, if we set $\Lambda = -\frac{377600k^2}{7803}$, the result is the same as example 2 in Ref. [77].

TABLE I. The solutions of the pure geometric $f(R)$ thick brane for $n = 3$, $n = 4$, and $n = 10$.

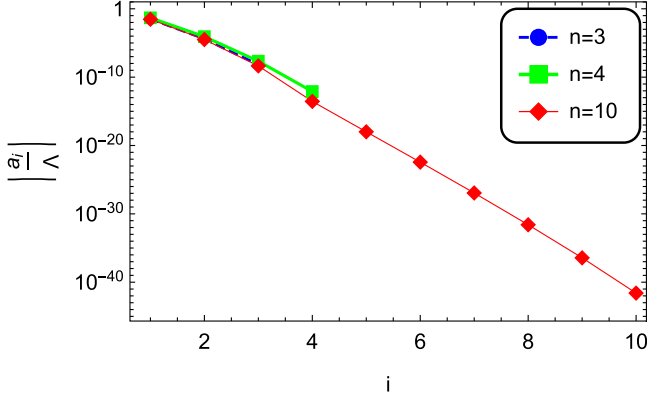| n	$n = 3$	$n = 4$	$n = 10$
δ	$\delta = 20$	$\delta = 14$	$\delta = \frac{114}{5}$
a_1	$-\frac{3147}{94400k^2}\Lambda \approx -0.0333\frac{\Lambda}{k^2}$	$-0.0478\frac{\Lambda}{k^2}$	$-0.0292\frac{\Lambda}{k^2}$
a_2	$\frac{249}{6041600k^4}\Lambda \approx 4.121 \times 10^{-5}\frac{\Lambda}{k^4}$	$2.488 \times 10^{-5}\frac{\Lambda}{k^4}$	$3.166 \times 10^{-5}\frac{\Lambda}{k^4}$
a_3	$-\frac{13}{1933312000k^6}\Lambda \approx -6.724 \times 10^{-9}\frac{\Lambda}{k^6}$	$-2.166 \times 10^{-8}\frac{\Lambda}{k^6}$	$-4.403 \times 10^{-9}\frac{\Lambda}{k^6}$
a_4		$7.927 \times 10^{-13}\frac{\Lambda}{k^8}$	$-2.834 \times 10^{-14}\frac{\Lambda}{k^8}$
a_5			$-1.002 \times 10^{-18}\frac{\Lambda}{k^{10}}$
a_6			$-3.689 \times 10^{-23}\frac{\Lambda}{k^{12}}$
a_7			$-1.130 \times 10^{-27}\frac{\Lambda}{k^{14}}$
a_8			$-2.550 \times 10^{-32}\frac{\Lambda}{k^{16}}$
a_9			$-3.684 \times 10^{-37}\frac{\Lambda}{k^{18}}$
a_{10}			$-2.530 \times 10^{-42}\frac{\Lambda}{k^{20}}$

FIG. 2. The coefficients $\left|\frac{a_i}{\Lambda}\right|$ in logarithmic coordinate. $n = 3$ for the dashed blue line, $n = 4$ for the green line, and $n = 10$ for the thin red line. The parameter is set to $k = 1$.
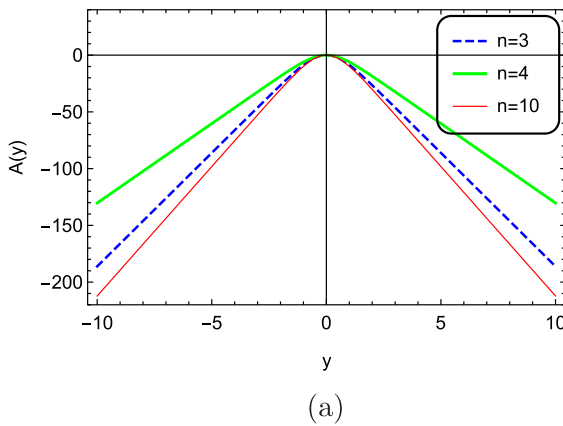
The pure geometric thick branes can be constructed, and the behaviors of the scalar curvature (15) at zero and infinity can be analyzed as follows:

$$
\begin{cases} R(y = 0) = 8\delta k^2, \\ R(y \to \infty) \to -20\delta^2 k^2. \end{cases} \quad (28)
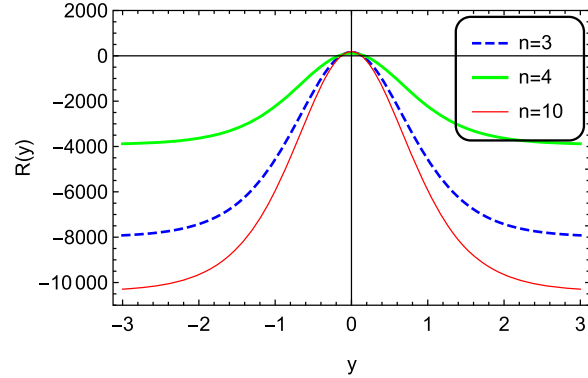$$

The shapes of $A(y)$ and $R(y)$ are shown in Figs. 3(a) and 3(b). We can find that both of $A(y)$ and $R(y)$ are smooth of the extra dimensional and $R(y)$ tends to a constant $-20\delta^2 k^2$ at infinity.

III. TENSOR PERTURBATION AND THE LOCALIZATION OF GRAVITY ON THE THICK $f(R)$ BRANES

The stability of the tensor perturbations of the gravity will be studied in this section. The small perturbations $h_{\mu\nu}$ are introduced into the metric [144]:

$$
ds^2 = \mathrm{e}^{2A(y)}(\eta_{\mu\nu} + h_{\mu\nu})dx^\mu dx^\nu + dy^2, \quad (29)
$$

where $h_{\mu\nu} = h_{\mu\nu}(x^\rho, y)$ depend on all the spacetime coordinates. The following relations can be obtained immediately:

$$
\begin{aligned}
\delta R_{\mu\nu} = &-\frac{1}{2}(\widehat{\Box}h_{\mu\nu} + \partial_\mu\partial_\nu h - \partial_\nu\partial_\sigma h_\mu^\sigma - \partial_\mu\partial_\sigma h_\nu^\sigma) \\
&- 2\mathrm{e}^{2A}A'h'_{\mu\nu} - 3h_{\mu\nu}\mathrm{e}^{2A}A'^2 - \frac{1}{2}\mathrm{e}^{2A}h''_{\mu\nu} \\
&- \frac{1}{2}\mathrm{e}^{2A}A'\eta_{\mu\nu}h',
\end{aligned} \quad (30)
$$

$$
\delta R_{\mu 5} = \frac{1}{2}\partial_y(\partial_\lambda h_\mu^\lambda - \partial_\mu h), \quad (31)
$$

$$
\delta R_{55} = -\frac{1}{2}(2A'h' + h''), \quad (32)
$$

$$
\begin{aligned}
\delta R &= \delta(g^{\mu\nu}R_{\mu\nu}) \\
&= -\mathrm{e}^{-2A}\widehat{\Box}h + \mathrm{e}^{-2A}\partial_\mu\partial_\nu h^{\mu\nu} - 5A'h' - h'',
\end{aligned} \quad (33)
$$

where $\widehat{\Box} = \eta^{\mu\nu}\partial_\mu\partial_\nu$ is the 4D d'Alembert operator, and $h = \eta^{\mu\nu}h_{\mu\nu}$. The tensor perturbations satisfy the transverse-traceless (TT) condition $\partial_\mu h_\nu^\mu = h = 0$.

The perturbed Einstein equations can be expressed:

$$
\begin{aligned}
&\delta R_{MN}f_R + R_{MN}f_{RR}\delta R - \frac{1}{2}\delta g_{MN}f(R) \\
&- \frac{1}{2}g_{MN}f_R\delta R + \delta(g_{MN}\Box f_R) - \delta(\nabla_M\nabla_N f_R) = 0, \quad (34)
\end{aligned}
$$

where

(a)

(b)

FIG. 3. The shapes of $A(y)$ in (a) and $R(y)$ in (b) for different thick brane solutions. $n = 3$ for the dashed blue line, $n = 4$ for the green line, and $n = 10$ for the thin red line. The parameter is set to $k = 1$.

$$f_{RR} \equiv \frac{\mathrm{d}f_R}{\mathrm{d}R} = \frac{\mathrm{d}^2 f(R)}{\mathrm{d}R^2},$$

$$\delta(\nabla_M \nabla_N f_R) = (\partial_M \partial_N - \Gamma^P_{MN} \partial_P)(f_{RR}\delta R) - \delta\Gamma^P_{MN} \partial_P f_R,$$

$$(35)$$

$$\delta(g_{MN}\Box f_R) = \delta g_{MN}\Box f_R + g_{MN}\delta g^{AB}(\nabla_A \nabla_B f_R)$$
$$+ g_{MN} g^{AB}\delta(\nabla_A \nabla_B f_R). \quad (36)$$

By substituting the Eqs. (30)–(33) into the Eq. (34), the perturbed Einstein equations can be simplified:

$$(e^{-2A}\widehat{\Box}h_{\mu\nu} + 4A'h'_{\mu\nu} + h''_{\mu\nu})f_R + h'_{\mu\nu}f'_R = 0, \quad (37)$$

or, we can have a more simpler form

$$\Box h_{\mu\nu} - \frac{f'_R}{f_R}\partial_y h_{\mu\nu} = 0. \quad (38)$$

By following the method given in Refs. [3,22], a coordinate transformation can be introduced

$$dz = e^{-A(y)}dy, \quad (39)$$

and the conformal flat metric can be taken:

$$ds^2 = e^{2A(z)}(\eta_{\mu\nu}dx^\mu dx^\nu + dz^2). \quad (40)$$

By using the coordinate transformation Eq. (39), the perturbed Einstein equations Eq. (38) are rewritten as:

$$\left[\partial_z^2 + \left(3\partial_z A + \frac{\partial_z f_R}{f_R}\right)\partial_z + \widehat{\Box}\right]h_{\mu\nu} = 0. \quad (41)$$

By doing the KK decomposition

$$h_{\mu\nu}(x^\rho, z) = e^{-\frac{3}{2}A}f_R^{-\frac{1}{2}}\epsilon_{\mu\nu}(x^\rho)\psi(z), \quad (42)$$

a Schrödinger-like equation for the KK modes $\psi(z)$ can be reexpressed

$$[-\partial_z^2 + W(z)]\psi(z) = m^2\psi(z), \quad (43)$$

where the effective potential $W(z)$ is

$$W(z) = \frac{9}{4}(\partial_z A)^2 + \frac{3}{2}\partial_z^2 A$$
$$+ \frac{3}{2}\frac{\partial_z A \partial_z f_R}{f_R} - \frac{1}{4}\frac{(\partial_z f_R)^2}{f_R^2} + \frac{\partial_z^2 f_R}{f_R}. \quad (44)$$

The above Eq. (44) can be factorized as

$$QQ^\dagger\psi(z) = m^2\psi(z) \quad (45)$$

with

$$Q = +\partial_z + \left(\frac{3}{2}\partial_z A + \frac{1}{2}\frac{\partial_z f_R}{f_R}\right), \quad (46)$$

$$Q^\dagger = -\partial_z + \left(\frac{3}{2}\partial_z A + \frac{1}{2}\frac{\partial_z f_R}{f_R}\right), \quad (47)$$

which ensures that there is no gravitational mode with $m^2 < 0$ and the braneworld solutions are stable against the tensor perturbations. However, the scalar perturbations are still not clear because of the higher derivatives in the perturbation equations. It is well known that a pure $f(R)$ gravity is conformally equivalent to a theory with a minimally coupled scalar in Einstein's gravity [131]. By following the method given by in Ref. [77], our solutions are stable against the small linear metric perturbations, including tensor, vector, and scalar perturbations, in the Einstein frame.

For Eq. (43), the zero mode with $m = 0$ is

$$\psi_{(0)}(z) = N_G e^{\frac{3}{2}A(z)}f_R^{\frac{1}{2}}(z), \quad (48)$$

where N_G is the normalization constant, and the $\psi_{(0)}(z)$ satisfies the normalizable condition

$$\int_{-\infty}^{+\infty} |\psi_{(0)}(z)|^2 dz = 1. \quad (49)$$

The coordinate transformation Eq. (39) can be rewritten as follows:

$$z = \int e^{-A(y)}dy = \int \cosh^\delta(ky)dy. \quad (50)$$

However, the above equation cannot be analytically calculated for an arbitrary δ, and it is also difficult to directly get the analytical expressions for the effective potential $W(z)$ and the zero mode $\psi_{(0)}(z)$ under the conformal coordinate z. So the solutions under the coordinate y can be calculated firstly, and the numerical solutions under the conformal coordinate z can also be obtained.

By using the relation

$$e^{-A(y)} \xrightarrow{y \to +\infty} 2^{-\delta}e^{\delta ky}, \quad (51)$$

the asymptotic behavior of the relation between z and y can be analyzed

$$z \xrightarrow{y \to +\infty} \frac{1}{2^\delta \delta k}e^{\delta ky}. \quad (52)$$

We can solve the asymptotic behavior of the relation between y and z for z tends to infinity
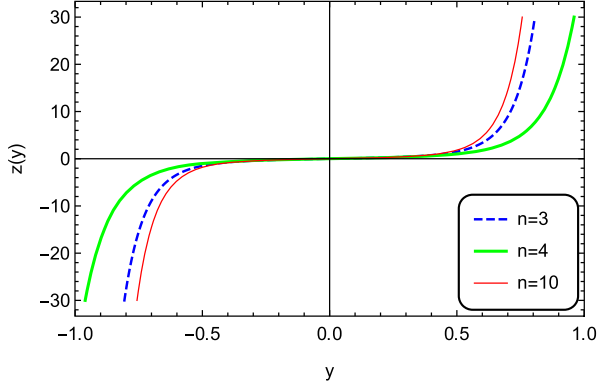
FIG. 4.   The relation between z and y. $n = 3$ for the dashed blue line, $n = 4$ for the green line, and $n = 10$ for the thin red line. The parameter is set to $k = 1$.
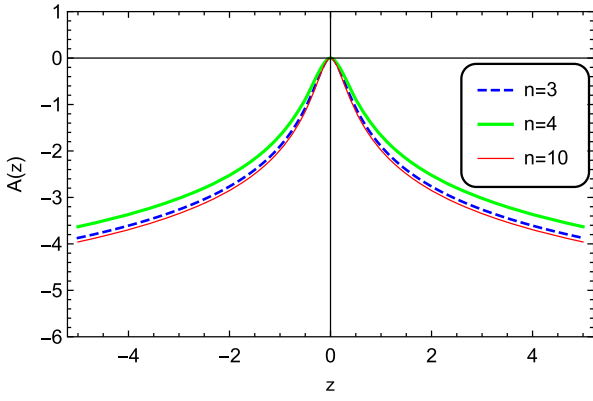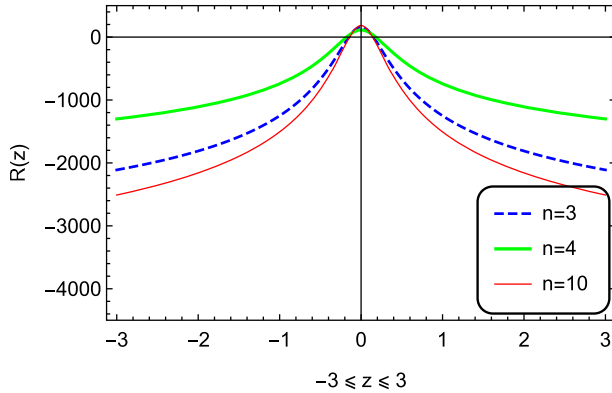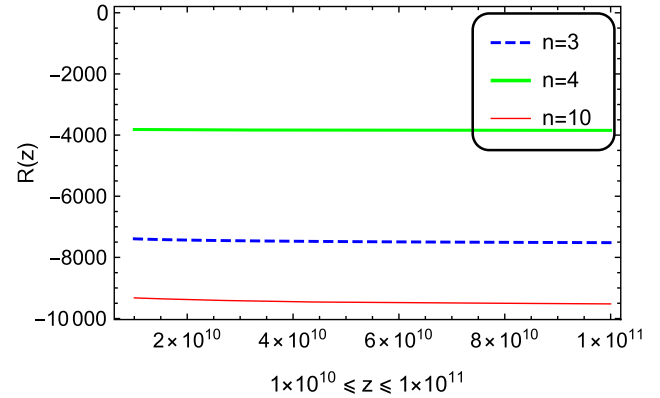

FIG. 5.   The shapes of $A(z)$ for different solutions. $n = 3$ for the dashed blue line, $n = 4$ for the green line, and $n = 10$ for the thin red line. The parameter is set to $k = 1$.

$$y \xrightarrow{y \to +\infty} \frac{1}{\delta k} \ln(2^{\delta} \delta k z). \tag{53}$$

And the relations between z and y can be solved by numerical method, and shown in Fig. 4, when δ are the determined values given by $n = 3$, 4, 10 respectively.

Then the behavior of $A(z)$ and the scalar curvature $R(z)$ at $z = 0$ and $z \to \pm\infty$ can be analyzed respectively,

$$\begin{cases} A(z = 0) = 0 \\ A(z \to \pm\infty) \to -\ln(\delta k |z|) \end{cases}, \tag{54}$$

$$\begin{cases} R(z = 0) = 8\delta k^2 \\ R(z \to \pm\infty) \to -20\delta^2 k^2 + C_1 |z|^{-\frac{2}{\delta}} \end{cases} \tag{55}$$

with $C_1 = (8\delta k^2 + 20\delta^2 k^2)(\delta k)^{-\frac{2}{\delta}}$, and we can have conclusions that the warp factor e^{2A} tends to 0 and R tends to a constant $-20\delta^2 k^2$ for $z \to \pm\infty$. The numerical solutions of $A(z)$ and $R(z)$ are also solved and shown in Figs. 5 and 6.

Since there is no analytical expression for the effective potential $W(z)$ with respect to the coordinate z, the expression for it in the coordinate y can be expressed as follows:

$$\begin{aligned} W(z(y)) = {} & \frac{15}{4} \mathrm{e}^{2A(y)} A'^2(y) + \frac{3}{2} \mathrm{e}^{2A(y)} A''(y) \\ & + \frac{1}{2} \mathrm{e}^{2A(y)} \frac{4A'(y) f'_R + f''_R}{f_R} \\ & - \frac{1}{4} \mathrm{e}^{2A(y)} \left(\frac{f'_R}{f_R} \right)^2. \end{aligned} \tag{56}$$

(a)

(b)

FIG. 6.   The shapes of the scalar curvature $R(z)$ for different solutions. $n = 3$ for the dashed blue line, $n = 4$ for the green line, and $n = 10$ for the thin red line. The range of the coordinate is around zero for (a), and the range of the coordinate is far away from zero for (b). The parameter is set to $k = 1$.
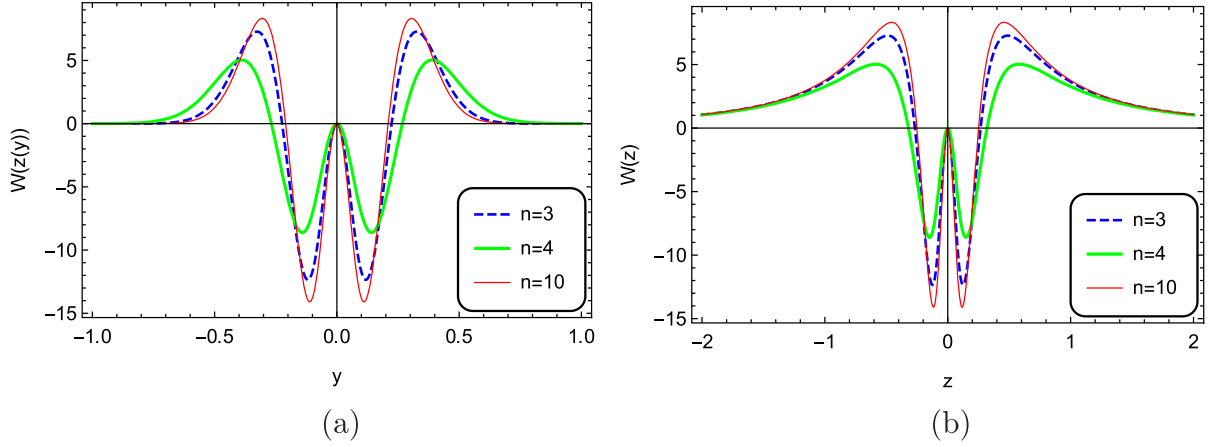
FIG. 7. The shapes of the potential $W(z(y))$ in 7(a) and $W(z)$ in 7(b) for different solutions. $n = 3$ for the dashed blue line, $n = 4$ for the green line, and $n = 10$ for the thin red line. The parameter is set to $k = 1$.

And the shapes of $W(z(y))$ are shown in Fig. 7(a). The numerically solution of $W(z)$ are shown in Fig. 7(b), which are similar to Fig. 7(a). The asymptotic behavior of these potentials tends zero at infinity. The height of the potential is related to the parameter δ decided by n. When $n = 10$ and $\delta = \frac{114}{5}$, the height of the potential is the tallest of all, and when $n = 4$ and $\delta = 14$, it is the lowest.

This potential supports a normalizable zero mode, and the normalization constant $N_{\rm G}$ satisfies the following condition:

$$
\begin{aligned}
1 &= \int_{-\infty}^{+\infty} |\psi_{(0)}(z)|^2 dz = N_{\rm G}^2 \int_{-\infty}^{+\infty} e^{3A(z)} f_R(z) dz \\
&= \frac{N_{\rm G}^2}{k} \int_{-\infty}^{+\infty} e^{2A(\omega)} f_R(\omega) d\omega,
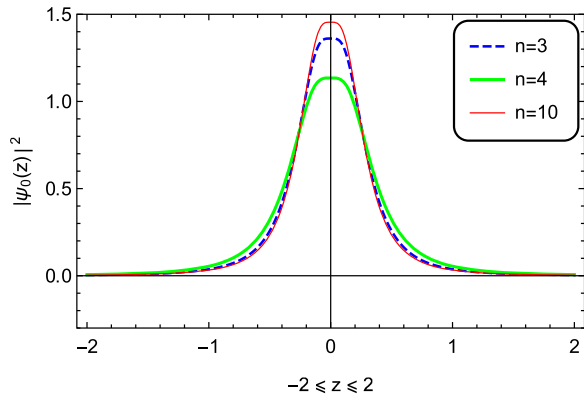\end{aligned}
\tag{57}
$$

FIG. 8. The shapes of the zero mode for gravity $|\psi_{(0)}(z)|^2$ for different solutions. $n = 3$ for the dashed blue line, $n = 4$ for the green line, and $n = 10$ for the thin red line. The parameter is set to $k = 1$.

where $\omega = ky$ and $dz = e^{-A} \frac{d\omega}{k}$. For our solutions, the above integration can be done analytically. For $n = 3$, the integration gives

$$
-\frac{N_{\rm G}^2}{k} \frac{3723736645632}{245251477631875k^2} \Lambda = 1,
\tag{58}
$$

and $N_{\rm G} \approx 8.115 k^{\frac{3}{2}}/\sqrt{-\Lambda}$. For $n = 4$ and $n = 10$, similarly, we can get $N_{\rm G} \approx 6.181 k^{\frac{3}{2}}/\sqrt{-\Lambda}$, and $N_G \approx 8.965 k^{\frac{3}{2}}/\sqrt{-\Lambda}$ respectively. Thus, the gravitational zero mode is normalizable and can be localized on the brane, which results in the familiar Newton's law on the brane. The shape of zero mode $|\psi_{(0)}(z)|^2$ is shown in Fig. 8. There is a platform for the gravitational zero mode around zero, so the zero mode is localized near zero.

Starting from $m^2 > 0$, the continuum of the massive KK modes might lead to a correction to the Newtonian potential on the brane. As have been addressed in Ref. [27], if the potential $\lim_{z \to \infty} W(z) = \frac{\beta(\beta+1)}{z^2}$, the massive modes will contribute a correction $\Delta U \propto 1/r^{2\beta}$ to the Newton's law at large distance (see also [46]). For our solutions, the asymptotic behavior of $z^2 W(z)$ with $z \to \infty$ can be analytically obtained. Instead of writing down the explicit expressions, it is shown in Fig. 9 that for our solutions $\lim_{z \to \infty} z^2 W(z) = \frac{15)}{4}$, namely $\beta = 3/2$. Thus, the corrections to the Newtonian potential $\Delta U \propto 1/r^3$ are suppressed at large r for the braneworld.

Note that for KK modes with $0 < m^2 < W_{\max}(z)$, there might exist some resonant KK modes which tend to plane waves when $z \to \infty$ and cannot be normalized for this type potential $W(z)$ [52]. Here $W_{\max}(z)$ is the maximum of the potential. However, according to the numerical calculation, there exists no resonant state.
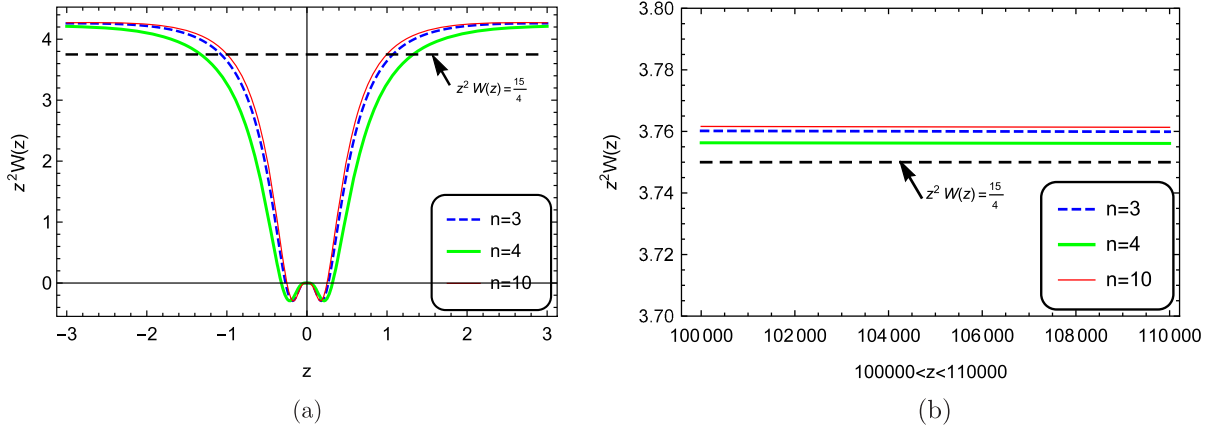
FIG. 9.   The shapes of $z^2W(z)$ for different solutions. $n = 3$ for the dashed blue line, $n = 4$ for the green line, and $n = 10$ for the thin red line. The parameter is set to $k = 1$.

IV. LOCALIZATION OF SPIN-0 SCALAR FIELDS ON THE THICK $f(R)$ BRANES

In this section, we will investigate the localization of scalar field on the thick $f(R)$ branes. We start with the action of a 5D massless scalar field:

$$S_0 = \int d^5x \sqrt{-g}\left[-\frac{1}{2}g^{MN}\partial_M\Phi\partial_N\Phi\right], \qquad (59)$$

and the equation of motion from the above action (59) is read as:

$$\frac{1}{\sqrt{-g}}\partial_M(\sqrt{-g}g^{MN}\partial_N\Phi) = 0. \qquad (60)$$

Using the conformal metric (40), and introducing the KK decomposition

$$\Phi(x^\mu, z) = \sum_\theta \phi_\theta(x^\mu)\chi_\theta(z)e^{-\frac{3}{2}A}, \qquad (61)$$

we can get the 4D Klein-Gordon equation

$$\frac{1}{\sqrt{-\hat{g}}}\partial_\mu(\sqrt{-\hat{g}}\eta^{\mu\nu}\partial_\nu)\phi_\theta = m_\theta^2\phi_\theta, \qquad (62)$$

where $\hat{g} = \det(\eta_{\mu\nu})$ is the determinant of the 4D effective metric, and the Schrödinger-like equation of the scalar KK modes respect to the extra dimensional coordinate

$$[-\partial_z^2 + V_0(z)]\chi_\theta(z) = m_\theta^2\chi_\theta(z), \qquad (63)$$

where m_θ is the mass of the θth KK mode of the scalar field, and the potential is given by:

$$V_0(z) = \frac{3}{2}\partial_z^2 A + \frac{9}{4}(\partial_z A)^2. \qquad (64)$$

The scalar KK modes should satisfy the following orthogonal normalization conditions:

$$\int_{-\infty}^{\infty} dz\chi_\theta(z)\chi_\sigma(z) = \delta_{\theta\sigma}, \qquad (65)$$

and the action (59) of the 5D free massless scalar field turns to the 4D effective action of a massless ($m_0 = 0$) and a series of massive ($m_\theta > 0$) scalar fields:

$$S_0 = \sum_\theta \int d^4x\sqrt{-g}\left[-\frac{1}{2}g^{\mu\nu}\partial_\mu\phi_\theta\partial_\nu\phi_\theta - \frac{1}{2}m_\theta^2\phi_\theta^2\right] \qquad (66)$$

By setting $m = 0$, the scalar zero mode can be solved from Eq. (63)

$$\chi_0(z) = N_S e^{\frac{3}{2}A(z)}, \qquad (67)$$

where N_S is the normalization constant given by

$$1 = \int_{-\infty}^{+\infty} |\chi_0(z)|^2 dz = N_S^2 \int_{-\infty}^{+\infty} e^{3A(z)}dz$$
$$= \frac{N_S^2}{k}\int_{-\infty}^{+\infty} e^{2A(\omega)}(\omega)d\omega. \qquad (68)$$
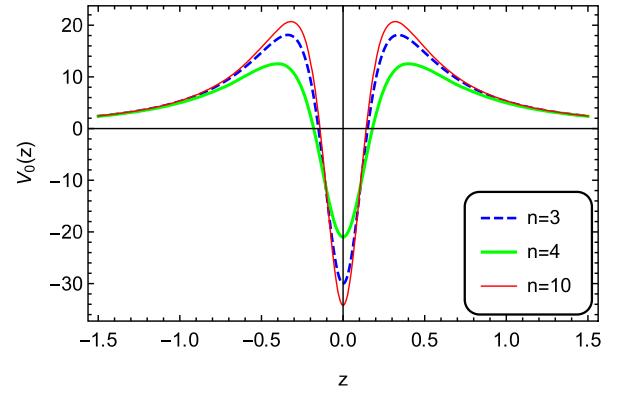

FIG. 10.   The shapes of the effective potential $V_0(z)$ for different solutions. $n = 3$ for the dashed blue line, $n = 4$ for the green line, and $n = 10$ for the thin red line. The parameter is set to $k = 1$.
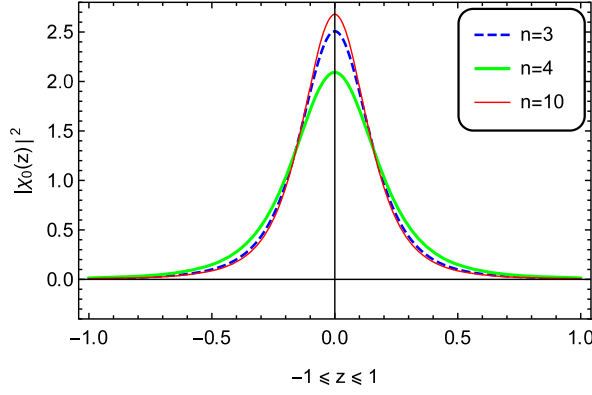
FIG. 11. The shapes of scalar field zero mode $|\chi_0(z)|^2$ for different solutions. $n = 3$ for the dashed blue line, $n = 4$ for the green line, and $n = 10$ for the thin red line. The parameter is set to $k = 1$.

When $n = 3$, $n = 4$, and $n = 10$, $N_S \approx 1.583\sqrt{k}$, $N_S \approx 1.446\sqrt{k}$, and $N_S \approx 1.637\sqrt{k}$ respectively. The zero mode of scalar can be localized on the brane.

Considering Eq. (54), the asymptotic behavior of $V_0(z)$ (64) and $\chi_0(z)$ (67) can be analyzed as follows:

$$\begin{cases} V_0(z = 0) = -\frac{3}{2}\delta k^2 \\ V_0(z \to \pm\infty) \to \frac{15}{4}|z|^{-2} \to 0, \end{cases} \quad (69)$$

$$\begin{cases} \chi_0(z = 0) = N_S \\ \chi_0(z \to \pm\infty) \to N_S(\delta k)^{-\frac{3}{2}}|z|^{-\frac{3}{2}}. \end{cases} \quad (70)$$

The numerical results of $V_0(z)$ and $|\chi_0(z)|^2$ are also shown in Figs. 10 and 11 respectively. We can have a conclusion that the zero mode of the scalar is localized at $z = 0$.

V. LOCALIZATION OF SPIN-1 VECTOR FIELDS ON THE THICK $f(R)$ BRANES

In this section, we will investigate the localization of vector fields on the thick $f(R)$ brane. We start with a 5D gauge invariant action for a vector field coupled to the scalar curvature [83]

$$S_1 = -\frac{1}{4}\int d^5x\sqrt{-g}g_V(R)g^{MN}g^{RS}F_{MR}F_{NS}, \quad (71)$$

where $F_{MN} = \partial_M A_N - \partial_N A_M$ is the field strength tensor, and $g_V(R)$ is the function of scalar curvature R. Setting $g_V(R) = 1$, the action of the 5D free vector field can be recovered. The equation of motion is read as follows:

$$\frac{1}{\sqrt{-g}}\partial_M(\sqrt{-g}g_V(R)g^{MN}g^{RS}F_{NS}) = 0. \quad (72)$$

Using the conformal metric (40), introducing the following general KK decomposition:

$$A_\mu(x^\lambda, z) = \sum_\theta a_\mu^{(\theta)}(x^\lambda)\rho_\theta(z)e^{-\frac{A}{2}}(g_V(R))^{-\frac{1}{2}}, \quad (73)$$

and choosing the gauge freedom $A_5 = 0$, the vector KK modes $\rho_\theta(z)$ should satisfy the following Schrödinger-like equation:

$$[-\partial_z^2 + V_1(z)]\rho_\theta(z) = m_\theta^2\rho_\theta(z), \quad (74)$$

where the effective potential $V_1(z)$ is

$$V_1(z) = \frac{1}{2}\partial_z^2 A + \frac{1}{4}(\partial_z A)^2$$
$$+ \frac{\partial_z A\partial_z g_V(R)}{2g_V(R)} + \frac{\partial_z^2 g_V(R)}{2g_V(R)} - \frac{(\partial_z g_V(R))^2}{4(g_V(R))^2}. \quad (75)$$

The full 5D action (71) can be reduced to the 4D effective action for a massless and series of massive vectors

$$S_1 = \sum_\theta \int d^4x\sqrt{-\hat{g}}\left(-\frac{1}{4}\eta^{\mu\alpha}\eta^{\nu\beta}f_{\mu\nu}^{(\theta)}f_{\alpha\beta}^{(\theta)}\right.$$
$$\left. - \frac{1}{2}m_\theta^2\eta^{\mu\nu}a_\mu^{(\theta)}a_\nu^{(\theta)}\right), \quad (76)$$

when integrated over the extra dimension, with the requirement that Eq. (74) is satisfied and the following ortho-normalization conditions are obeyed:

$$\int_{-\infty}^{\infty}\rho_\theta(z)\rho_\sigma(z)dz = \delta_{\theta\sigma}. \quad (77)$$

By setting $m = 0$, the solution of zero mode of the KK modes can be calculated:

$$\rho_0(z) = N_V e^{\frac{1}{2}A(z)}(g_V(R(z)))^{\frac{1}{2}}, \quad (78)$$

where N_V is the normalization constant given by

$$1 = \int_{-\infty}^{+\infty}|\rho_0(z)|^2 dz = N_V^2\int_{-\infty}^{+\infty}e^{A(z)}g_V(R(z))dz$$
$$= \frac{N_V^2}{k}\int_{-\infty}^{+\infty}g_V(R(\omega))d\omega. \quad (79)$$

Next we will investigate the relation between the coupling with the gravity and the localization mechanism of the KK modes for the vector field.

A. Without the coupling: $g_V(R) = 1$

First, we do not introduce the coupling between the vector field and the background spacetime, i.e., $g_V(R) = 1$. From Eq. (75), the potential of the vector can be reduced to

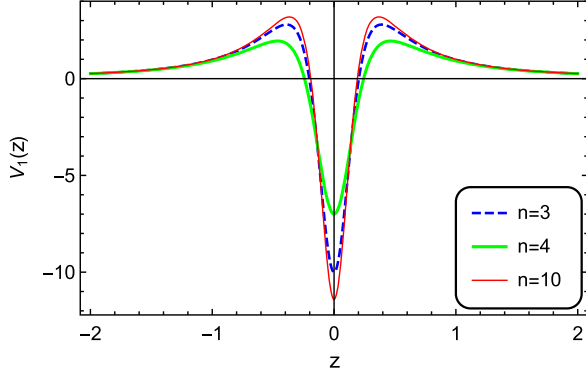$$V_1(z) = \frac{1}{2}A'' + \frac{1}{4}A'^2, \quad (80)$$

FIG. 12. The shapes of vector field effective potential $V_1(z)$ without coupling term for different solutions. $n = 3$ for the dashed blue line, $n = 4$ for the green line, and $n = 10$ for the thin red line. The parameter is set to $k = 1$.

and the asymptotic behavior of $V_1(z)$ at $z = 0$ and $z \to \infty$ can be analyzed as follows

$$\begin{cases} V_1(z=0) = \frac{1}{2}\delta k^2 \\ V_1(z \to \pm\infty) \to \frac{3}{4}z^{-2} \to 0. \end{cases} \tag{81}$$

The shapes of $V_1(z)$ for the thick brane solutions are shown in Fig. 12 by numerical method.

The zero mode (78) can also be reduced to

$$\rho_0(z) = N_V e^{\frac{1}{2}A}, \tag{82}$$

and the asymptotic behavior of $\rho_0(z)$ has be calculated

$$\begin{cases} \rho_0(z=0) = N_V \\ \rho_0(z \to \pm\infty) \to \frac{1}{\sqrt{\delta k}}z^{-\frac{1}{2}} \to 0. \end{cases} \tag{83}$$

From Eqs. (79) and (83), it is clear that the zero mode does not satisfy the normalization constant, i.e.,

$$\int_1^\infty |\rho_0(z)|^2 dz \approx \int_1^\infty \frac{1}{z}dz \to \infty. \tag{84}$$

Therefore the zero mode $\rho_0(z)$ Eq. (82) cannot be localized on the brane without the coupling between the vector and the gravity. The situation is the same as the RS model.

B. With the coupling: $g_V(R) = (1 + \frac{R}{20\delta^2 k^2})^q$

In order to localization of the zero mode of the vector field, the coupling between the vector and the gravity must be introduced, and the following simple form is chosen in this paper:

$$g_V(R) = \left(1 + \frac{R}{20\delta^2 k^2}\right)^q, \tag{85}$$

where q is coupling coefficient.

By using Eq. (75), the effective potential can be given by

$$V_1(z) = \frac{A''}{2} + \frac{A'^2}{4} + \frac{q(A'R\prime + R\prime)}{40k^2\delta^2 + 2R} + \frac{q(q-2)R'2}{4(20k^2\delta^2 + R)^2}, \tag{86}$$

and the asymptotic behaviors of $V_1(z)$ at zero and infinity are

$$\begin{cases} V_1(z=0) = -\frac{1}{2}(\delta + 2q)k^2 \\ V_1(z \to \infty) \to (\frac{3}{4} + \frac{2q}{\delta} + \frac{q^2}{\delta^2})z^{-2}. \end{cases} \tag{87}$$

The zero mass mode can also be given by

$$\rho_0 = N_V e^{\frac{1}{2}A(z)}\left(1 + \frac{R}{20k^2\delta^2}\right)^{\frac{q}{2}}, \tag{88}$$

and the asymptotic behaviors of the zero mode $\rho_0(z)$ at $z = 0$ and $z \to \infty$ are

$$\begin{cases} \rho_0(z=0) = N_V(\frac{5\delta+2}{5\delta})^{\frac{q}{2}} \\ \rho_0(z \to \infty) \to N_V(\frac{5\delta+2}{5\delta})^{\frac{q}{2}}(\delta k)^{-\frac{\delta+2q}{2\delta}}z^{-\frac{\delta+2q}{2\delta}}. \end{cases} \tag{89}$$

For the purpose of trapping the zero mode of the vector field on the brane, the normalization condition (79) should be satisfied, i.e.,

$$\int_1^\infty \rho_0^2(z \to +\infty)dz \approx \int_1^\infty z^{-1-2\frac{q}{\delta}}dz < \infty, \tag{90}$$

which require that the coupling coefficient must be positive $q > 0$. In this paper, we will investigate the effects of the coupling coefficient q on the localization of the vector KK modes, so here set $q = \frac{1}{2}\delta, 5\delta, 10\delta, 20\delta$. The numerical solutions of the potential $V_1(z)$ for the $n = 3$ thick brane are shown Fig. 13. It is clear that the potentials have a negative well around $z = 0$ and have two symmetrical barriers at both sides of the origin of the extra
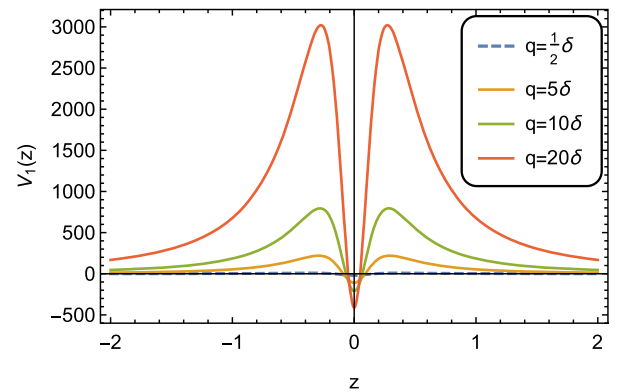

FIG. 13. The shapes of the effective potential for the vector fields $V_1(z)$ with coupling term for different values of the coupling coefficient q. The parameters are set to $n = 3$ and $k = 1$.
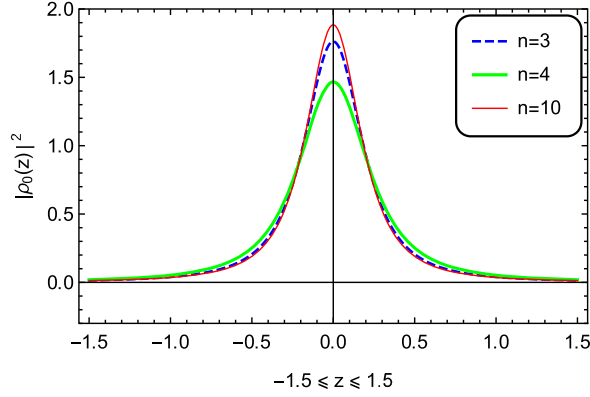
FIG. 14. The shapes of vector field zero modes $|\rho_0(z)|^2$ with the coupling coefficient $q = \frac{\delta}{2}$ for different solutions. $n = 3$ for the dashed blue line, $n = 4$ for the green line, and $n = 10$ for the thin red line. The parameter is set to $k = 1$.

dimension, which increased with the coupling coefficient q. For the case of $n = 4$ and $n = 10$, the potentials are similar to $n = 3$. When $q = \frac{\delta}{2}$, the numerical results of the vector zero mode for $n = 3$, $n = 4$, and $n = 10$ have been also shown in Fig. 14. Generally, this type of potential implies that there may exist resonant states, which tend to plane waves when $z \to \infty$ and cannot be normalized. Following the method presented in Refs. [105,109,110,152], the relative probability function of a resonance on the brane is defined as follows:

$$P_{\mathrm{V}}(m^2) = \frac{\int_{-z_{\mathrm{b}}}^{z_{\mathrm{b}}} |\rho(z)|^2 dz}{\int_{-z_{\mathrm{max}}}^{z_{\mathrm{max}}} |\rho(z)|^2 dz}, \qquad (91)$$

where $2z_{\mathrm{b}}$ is approximately the width of the thick brane, and $z_{\mathrm{max}} = 10z_{\mathrm{b}}$. It is clear that the KK modes are

TABLE II. The mass, width, and lifetime of resonant KK modes of the vector with $k = 1$.

| n	δ	q	V_1^{max}	θ	m^2	m	Γ	τ
3	20	5δ	220.1707	1	173.1216	13.1575	0.2574	3.8840
		10δ	794.7859	1	377.0040	19.4165	6.092×10^{-4}	1.641×10^3
				2	659.3324	25.6774	0.1214	8.2327
				3	829.4739	28.8005	1.4998	0.6667
		20δ	3.020×10^3	1	778.1259	27.8949	1.431×10^{-11}	6.984×10^{10}
				2	1.470×10^3	38.3434	6.533×10^{-7}	1.530×10^6
				3	2.070×10^3	45.5006	3.880×10^{-4}	2.577×10^3
				4	2.567×10^3	50.6670	0.0273	36.5568
				5	2.931×10^3	54.1458	0.4101	2.4379
				6	3.176×10^3	56.3604	2.4695	0.4049
4	14	5δ	152.5827	1	120.7882	10.9903	0.2455	4.0724
		10δ	550.7041	1	263.5687	16.2348	$6,529 \times 10^{-4}$	1.531×10^3
				2	459.9604	21.4466	0.1200	8.3271
				3	581.1552	24.1071	1.5808	0.6325
		20δ	2.092×10^3	1	544.3748	23.3318	1.988×10^{-11}	5.028×10^{10}
				2	1.027×10^3	32.0602	8.152×10^{-7}	1.226×10^6
				3	1.446×10^3	38.0281	4.501×10^{-4}	2.221×10^3
				4	1.790×10^3	42.3200	0.0295	33.8816
				5	2.042×10^3	45.1897	0.4127	2.4229
				6	2.230×10^3	47.2321	3.6694	0.2725
10	$\frac{114}{5}$	5δ	251.7237	1	197.5419	14.0549	0.2653	3.7686
		10δ	908.7305	1	429.9404	20.7350	6.001×10^{-4}	1.666×10^3
				2	752.3325	27.4286	0.1222	8.1773
				3	945.6910	30.7520	1.5185	0.6585
		20δ	3.453×10^3	1	887.2097	29.7860	1.301×10^{-11}	7.686×10^{10}
				2	1.676×10^3	40.9470	6.170×10^{-7}	1.620×10^6
				3	2.361×10^3	48.5960	3.745×10^{-4}	2.670×10^3
				4	2.929×10^3	54.1234	0.0268	37.2132
				5	3.346×10^3	57.8474	0.4162	2.4025
				6	3.615×10^3	60.1269	2.5566	0.3911
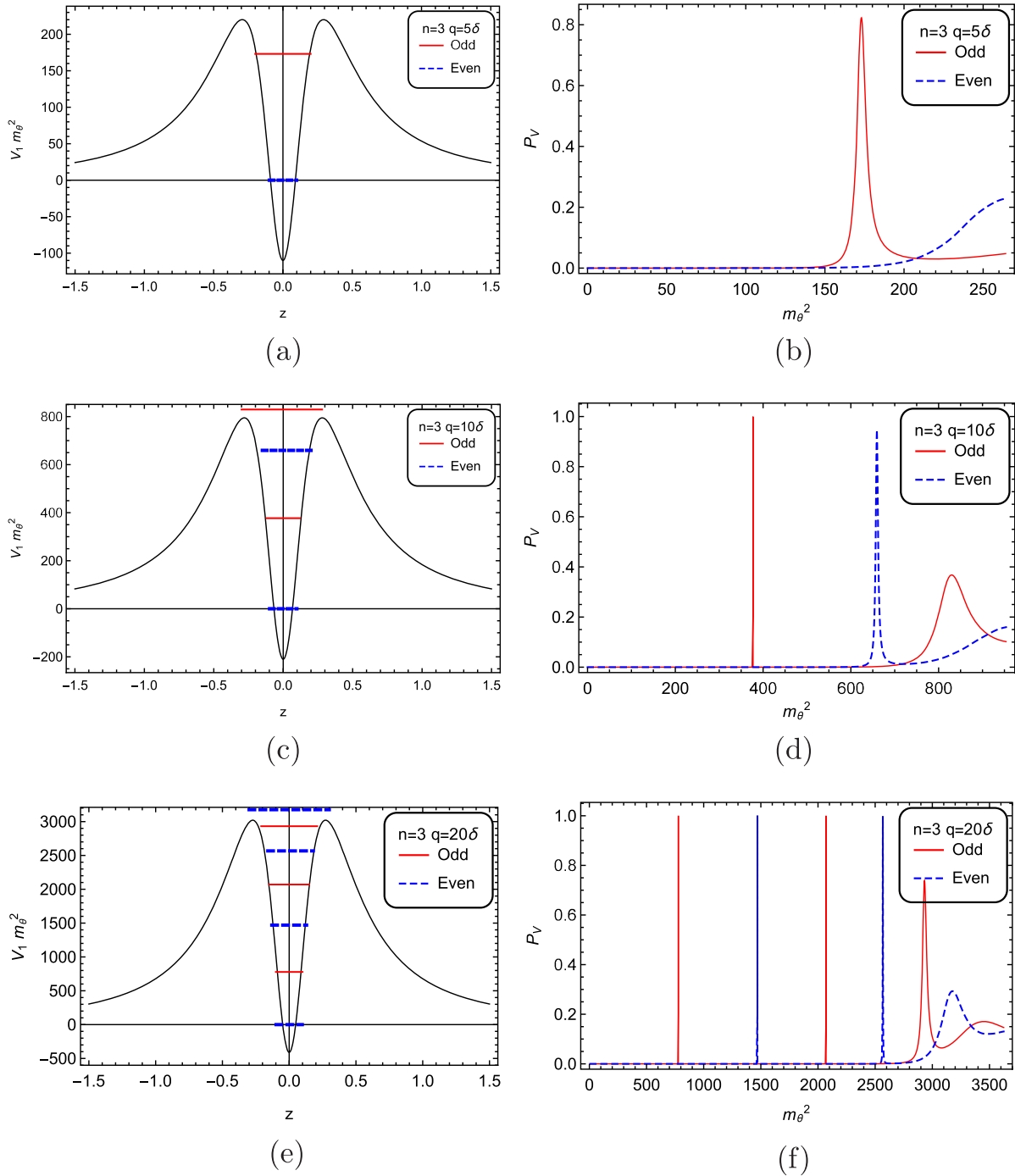
FIG. 15. The mass spectra, the effective vector potential V_1, and corresponding relative probability P_V with different coupling coefficient $q = 5\delta, 10\delta, 20\delta$. V_1 for the black line, the even parity KK mode for the blue line, and the odd parity KK mode for the red line. The parameters are set to $n = 3$ and $k = 1$.

approximately taken as plane waves and the corresponding probability $P_V(m^2)$ tend to $1/10$, when $m^2 \gg V_1^{\max}$ ($V_1^{\max}$ is the maximum value of the corresponding potential V_1). The lifetime τ of a resonant state is $\tau \sim \Gamma^{-1}$ with $\Gamma = \delta m$ being the full width at half maximum of the peak. Equation (74) can be solved by the numerical method, and we will set the

coupling coefficient q as different values $q = \frac{1}{2}\delta, 5\delta, 10\delta, 20\delta$, for each thick brane solution ($n = 3$, $n = 4$, and $n = 10$), respectively.

When $q = \frac{1}{2}\delta$, there is no resonant state vector KK mode for each thick brane solution. However, when $q = 5\delta$, there is one resonant KK mode for each thick brane solution, and
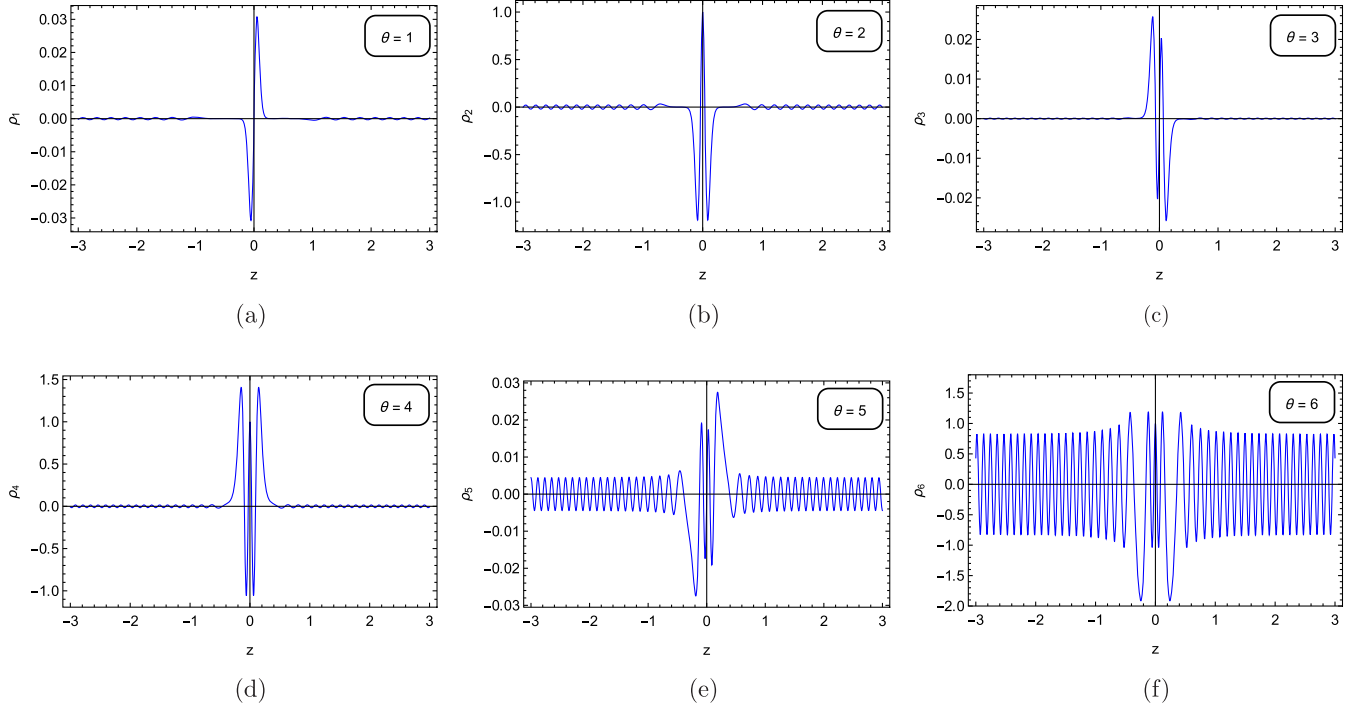
FIG. 16. The shapes of vector resonance KK modes with the coupling coefficient $q = 20\delta$. The parameters are set to $n = 3$ and $k = 1$.

the total number of resonant KK modes increases with the coupling coefficient q. The mass, width, and lifetime of the vector resonant KK modes with different values of q for each thick brane solution are listed in Table II.

For the case of $n = 3$ thick brane solution, the profiles of the relative probability P_V corresponding to different coupling coefficient q are shown in Fig. 15. In these figures, each peak corresponds to a resonant state, and the corresponding mass spectra with the effective potentials are also shown in Fig. 15. For the mass spectra of the vector KK modes, it can be seen that the ground state is zero mode (bound state), and all the massive KK modes are resonant KK modes. From Table II and Fig. 15(f), it is clear that there are six resonant KK modes when $q = 20\delta$, and all the resonant KK modes are shown in Fig. 16. So we can summarize that the vector KK zero mode can be localized on the pure geometric thick $f(R)$ brane, and the massive KK modes can be quasilocalized on the brane. For the other cases $n = 4(\delta = 14)$ and $n = 10(\delta = \frac{114}{5})$, the situation is similar to the case of $n = 3(\delta = 20)$. Furthermore, the coupling function $g_V(R)$ can also be set as other formulations and the property of the localization will be different. And the discussion in more detail has be investigated in Ref. [83].

VI. LOCALIZATION OF SPIN-1/2 FERMION FIELDS ON THE THICK $f(R)$ BRANES

In this section, the localization of Spin$-1/2$ fermion field on the thick $f(R)$ branes will be investigated,

and the 5D Dirac action of fermion can be expressed as

$$S_{\frac{1}{2}} = \int d^5 x \sqrt{-g} [\bar{\Psi} \Gamma^M (\partial_M + \omega_M) \Psi - \eta \bar{\Psi} \Gamma^M \partial_M g_f(R) \Psi],$$

(92)

where ω_M is the spin connection defined as

$$\omega_M = \frac{1}{4} \omega_M^{\bar{M} \bar{N}} \Gamma_{\bar{M}} \Gamma_{\bar{N}}$$

(93)

with

$$\omega_M^{\bar{M} \bar{N}} = \frac{1}{2} E^{N\bar{M}} (\partial_M E_N^{\bar{N}} - \partial_N E_M^{\bar{N}}) - \frac{1}{2} E^{N\bar{N}} (\partial_M E_N^{\bar{M}} - \partial_N E_M^{\bar{M}})$$
$$- \frac{1}{2} E^{P\bar{M}} E^{Q\bar{N}} E_M^{\bar{R}} (\partial_P E_{Q\bar{R}} - \partial_Q E_{P\bar{R}}).$$

(94)

The letters with barrier $\bar{M}, \bar{N}$ are the five dimensional local Lorentz indices and the vielbein $E_{\bar{M}}^M$ satisfies $E_{\bar{M}}^M E_{\bar{N}}^N \eta^{\bar{M} \bar{N}} = g^{MN}$. The relation between the gamma matrices Γ^M and $\Gamma^{\bar{M}} = (\Gamma^{\bar{\mu}}, \Gamma^{\bar{5}}) = (\gamma^{\bar{\mu}}, \gamma^{\bar{5}})$ is given by $\Gamma^M = E_{\bar{m}}^M \Gamma^{\bar{M}}$.

Here the coupling between Dirac fermion and background spacetime [129] $-\eta \bar{\Psi} \Gamma^M \partial_M g_f(R) \Psi$ with η coupling coefficient is introduced. Here we assume that the coupling coefficient η is positive.

Considering the conformally flat metric Eq. (40), the component of the spin connection is given by

$\omega_\mu = \frac{1}{2}(\partial_z A(z))\gamma_\mu\gamma_5$ and $\omega_5 = 0$. The equation of motion of the 5D Dirac fermion can be derived as

$$[\gamma^\mu\partial_\mu + \gamma^5(\partial_z + 2\partial_z A(z)) + \eta\partial_z g_{\text{f}}(R)]\Psi = 0. \quad (95)$$

The chiral decomposition for $\Psi(x,z)$ can be introduced,

$$\Psi(x,z) = e^{-2A(z)}\sum_\theta[\psi_{L_\theta}(x)L_\theta(z) + \psi_{R_\theta}(x)R_\theta(z)], \quad (96)$$

where $\Psi_{L_\theta} = -\gamma^5\Psi_{L_\theta}$ and $\Psi_{R_\theta} = \gamma^5\Psi_{R_\theta}$ are the left- and right-chiral components of the 4D Dirac fermion field, respectively.

By takeing the following orthonormalization conditions for the KK modes L_θ and R_θ

$$\int_{-\infty}^{\infty} L_\theta L_\sigma dz = \delta_{\theta\sigma}, \quad (97)$$

$$\int_{-\infty}^{\infty} R_\theta R_\sigma dz = \delta_{\theta\sigma}, \quad (98)$$

$$\int_{-\infty}^{\infty} L_\theta R_\theta dz = 0, \quad (99)$$

one can take the effective action of the 4D massless and massive Dirac fermions from the 5D Dirac action (92)

$$S_{\frac{1}{2}} = \sum_\theta\int d^4x\sqrt{-\hat{g}}\bar{\psi}_\theta[\gamma^\mu(\partial_\mu + \hat{\omega}_\mu) - m_\theta]\psi_\theta. \quad (100)$$

By introducing the chiral decomposition Eq. (96), the Schrödinger-like equations of motion for the left- and right-chiral fermion KK modes $L_\theta(z)$ and $R_\theta(z)$ can be obtained:

$$[-\partial_z^2 + V_{\text{L}}(z)]L_\theta(z) = m_\theta^2 L_\theta(z), \quad (101a)$$

$$[-\partial_z^2 + V_{\text{R}}(z)]R_\theta(z) = m_\theta^2 R_\theta(z), \quad (101b)$$

where the effective potentials $V_{\text{L,R}}(z)$ of the fermion KK modes are read as

$$V_{\text{L}}(z) = (\eta\partial_z g_{\text{f}}(R))^2 + \eta\partial_z^2 g_{\text{f}}(R), \quad (102a)$$

$$V_{\text{R}}(z) = (\eta\partial_z g_{\text{f}}(R))^2 - \eta\partial_z^2 g_{\text{f}}(R). \quad (102b)$$

By setting $m_\theta = 0$ in Eq. (101), the solution of zero modes L_0 and R_0 can be obtained

$$L_0 \propto e^{\int_0^z dz\eta\partial_z g_{\text{f}}(R)} = e^{\eta g_{\text{f}}(R(z))} \quad (103a)$$

$$R_0 \propto e^{-\int_0^z dz\eta\partial_z g_{\text{f}}(R)} = e^{-\eta g_{\text{f}}(R(z))}. \quad (103b)$$

From the above relations (103), it is impossible to make both massless left- and right-chiral KK modes to be localized on the brane at the same time, since when one is normalizable, the other one is not.

From Eqs. (101) and (102), it is clear that, if we do not introduce the coupling in the action (92), i.e., $\eta = 0$, the effective potentials for left- and right-chiral KK modes $V_{\text{L,R}}(z) = 0$ and both left- and right-chiral fermions cannot be localized on the thick brane, so the coupling term must be introduced. Moreover, since R is even function of z, $V_{\text{L,R}}(z)$ are naturally Z_2 even with respect to z. Here we set a simple formulation:

$$g_{\text{f}}(R) = -\frac{20\delta^2 k^2 + 8\delta k^2}{R + 20\delta^2 k^2}, \quad (104)$$

By using Eqs. (54), (55), and (104), the asymptotic behaviors of $V_{\text{L,R}}(z)$ at $z = 0$ and $z \to \infty$ are as follows

$$\begin{cases} V_{\text{L}}(z = 0) = -2\eta k^2, \\ V_{\text{L}}(z \to \infty) \to \frac{2\eta}{\delta^2}(1-\delta)z^{-2}, \end{cases} \quad (105)$$

$$\begin{cases} V_{\text{R}}(z = 0) = 2\eta k^2, \\ V_{\text{R}}(z \to \infty) \to \frac{2\eta}{\delta^2}(\delta-1)z^{-2}. \end{cases} \quad (106)$$

Considering the coupling formulation (104) and Eq. (103), for the positive coupling coefficient η and positive parameter δ and k, only left-chiral fermion zero mode may be localized on the brane. The asymptotic behavior of $L_0(z)$ is also given by

$$\begin{cases} L_0(z = 0) = N_L e^{-\eta}, \\ L_0(z \to \infty) \to N_L e^{-\eta C_L|z|^s}, \end{cases} \quad (107)$$

where N_L is a constant, $C_L = (\delta k)^{\frac{\delta}{2}} > 0$ and $s = \frac{\delta}{2} \geq \frac{\delta_{\min}}{2} = 7$ are positive constants, respectively. It is easy to see that the normalization condition of the left-chiral fermion zero mode is satisfied, and it can be localized on the brane.

Next, the effect of the coupling between fermion and background spacetime for the property of the localization will be investigated, so the coupling coefficient η will be taken different values: $\eta = 1, 50, 100$. This type potential implies that resonant left- and right-chiral KK modes may exist. Mimic to the case of vector, the fermion relative probabilities for finding the left- and right-chiral fermion resonant states with mass m can be defined as:

$$P_{\text{L,R}}(m^2) = \frac{\int_{-z_b}^{z_b}|L,R(z)|^2 dz}{\int_{-z_{\max}}^{z_{\max}}|L,R(z)|^2 dz}. \quad (108)$$
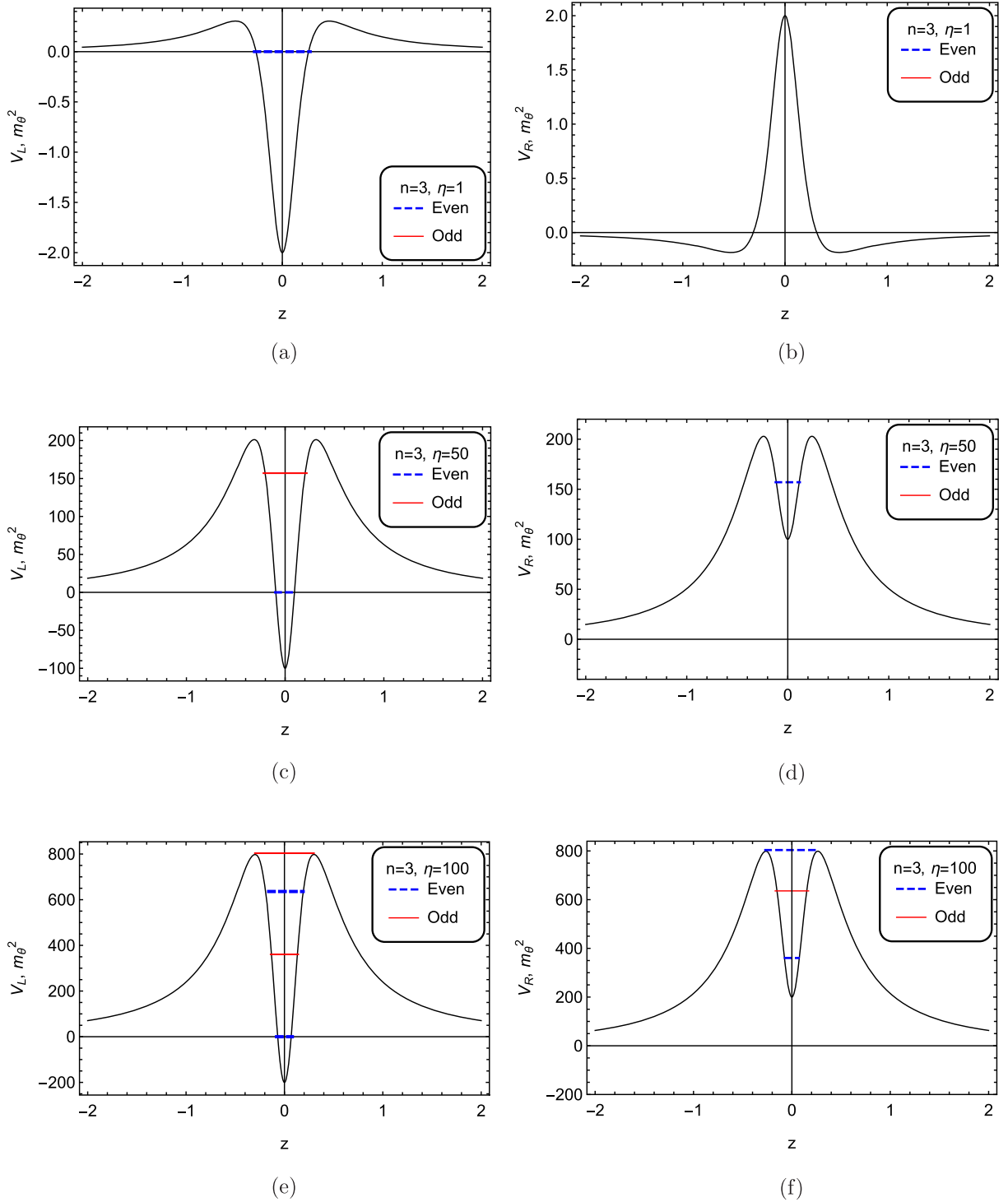
FIG. 17.   The mass spectra and the effective potentials of the left- and right-chiral fermions with different coupling coefficient $\eta = 1$, $\eta = 50$, and $\eta = 100$. The parameters are set to $n = 3$ and $k = 1$.

For the case of $n = 3$, when the coupling coefficient $\eta = 1$, the effective potentials and the mass spectra for the left- and right-chiral fermion KK modes are shown in Figs. 17(a) and 17(b). Only the left-chiral fermion zero mode (bound state) can be localized on the brane.

When the coupling coefficient $\eta = 50$, the effective potentials and the mass spectra for the left- and right-chiral fermion KK modes are shown in Figs. 17(c) and 17(d). For the left-chiral fermion KK modes, there is only one bound zero mode and one massive resonant
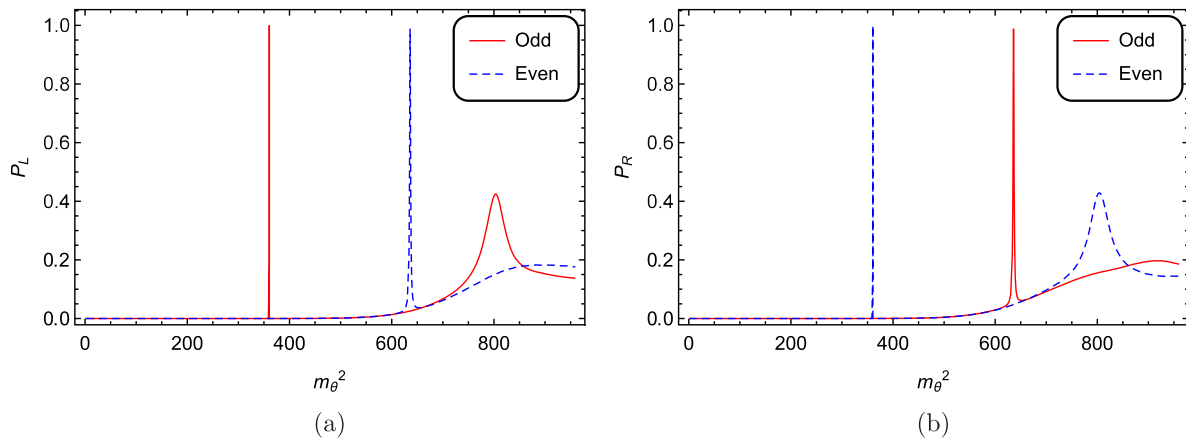
FIG. 18. The shapes of the relative probability $P_L(m^2)$ for the left-chiral fermion and $P_R(m^2)$ for right-chiral fermion resonant. The parameters are set to $\eta = 100$, $n = 3$, and $k = 1$.
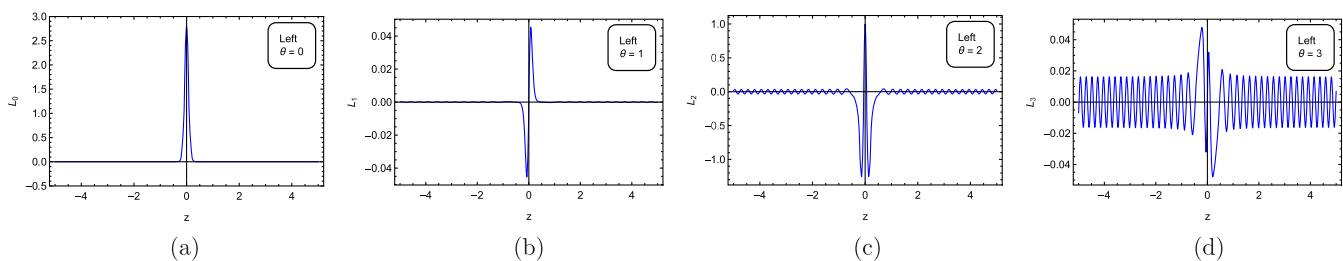

FIG. 19. The shapes of the left-chiral fermion KK modes, which is set to $\eta = 100$, $n = 3$, and $k = 1$.

KK mode, which is an even-parity. However, for the right-chiral fermion KK mode, there is only one massive resonant KK mode, which is an odd-parity. Both the mass of the left- and right-chiral fermion KK modes are the same. In fact, these conclusions are originated from the coupled equations of the left- and right-chiral fermions. When $\eta = 100$, the effective potentials and the mass spectra for the left- and right-chiral fermion KK modes are shown in Figs. 17(e) and 17(f). The profiles of the relative probability $P_{L,R}(m^2)$ are shown in Figs. 18(a) and 18(b), respectively. And the left- and right-chiral fermion KK modes are shown in Figs. 19 and 20. So we can summarize that the 4D massless left-chiral fermion can be localized on the brane, and the 4D massive Dirac fermions can also be quasilocalized on the brane, which consist of the pairs of coupled left- and right-chiral KK modes with different parities. The total number of resonant KK modes increases with the coupling coefficient η.

For the cases of $n = 4$ and $n = 10$, the situation is similar to the case of $n = 3$, and the mass, width, and lifetime of the left- and right-chiral fermion KK resonant modes are listed in Table III.

Furthermore, the coupling function $g_f(R)$ can also be set as other formulations and the property of the localization will be different. And the discussion in more detail has been investigated in Ref. [129].
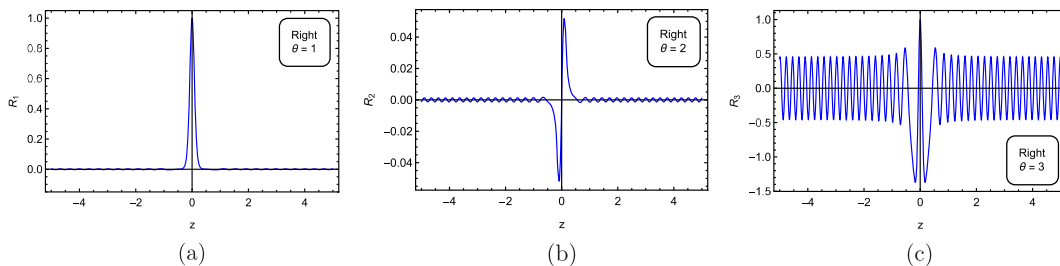

FIG. 20. The shapes of the right-chiral fermion KK modes, which is set to $\eta = 100$, $n = 3$, and $k = 1$.

TABLE III. The mass, width, and lifetime of resonant KK modes of the fermions with the parameter $k = 1$.

n	η	Chrial	Height of $V_{L,R}$	θ	m^2	m	Γ	τ
3	50	Left	201.3102	1	157.0089	12.5303	0.1732	5.7749
		Right	202.9641	1	156.9938	12.5297	0.1801	5.5527
	100	Left	798.2219	1	360.5018	18.9869	9.592×10^{-5}	1.042×10^4
				2	635.9341	25.2177	0.0464	21.5500
				3	803.5692	28.3473	1.2032	0.8311
		Right	798.9972	1	360.5020	18.9868	9.555×10^{-5}	1.046×10^4
				2	635.9326	25.2177	0.0470	21.2549
				3	803.7101	28.3497	1.3213	0.7568
4	50	Left	296.0509	1	172.5166	13.1345	0.0057	173.6421
				2	281.7977	16.7868	0.4054	2.4664
		Right	296.7473	1	172.5166	13.1345	0.0058	172.3199
				2	281.6335	16.7819	0.4227	2.3652
	100	Left	1.179×10^3	1	373.4193	19.3240	1.844×10^{-9}	5.421×10^8
				2	691.9976	26.3058	4.681×10^{-5}	2.136×10^4
				3	950.5699	30.8313	0.0113	88.4840
				4	1.134×10^3	33.6808	0.2806	3.5632
		Right	1.179×10^3	1	373.4196	19.3240	1.868×10^{-9}	5.353×10^8
				2	691.9974	26.3058	4.647×10^{-5}	2.151×10^4
				3	950.5701	30.8313	0.0114	87.4471
				4	1.134×10^3	33.6800	0.2929	3.4134
10	50	Left	175.4931	1	149.2316	12.2160	0.3738	2.6751
		Right	177.7526	1	149.0260	12.2076	0.4045	2.4718
	100	Left	694.0240	1	354.2681	18.8220	0.0010	929.1899
				2	606.2331	24.6218	0.1903	5.2540
		Right	695.0366	1	354.2683	18.8220	0.0011	909.9818
				2	606.3846	24.6248	0.1982	5.0438

VII. CONCLUSION AND DISCUSSION

In this paper, we investigate a pure geometric thick $\mathcal{M}_4$ brane, embedded in a AdS$_5$ spacetime, in general $f(R)$ gravity theory. Here, the form of $f(R)$ is set as $f(R) = \sum_{i=1}^{n} a_i R^i + \Lambda$, and any background scalar has not been introduced. For the pure geometric thick $\mathcal{M}_4$ brane, the parameter n must be satisfied $n \geq 3$, and for a certainty value of n, a thick brane solution can be obtained. In this paper, the solutions of the $\mathcal{M}_4$ brane for $n = 3$, $n = 4$, and $n = 10$, have been studied, and found that the solutions are stable against tensor perturbations. Moreover, we investigate the localization of gravity and various bulk matter fields on the branes.

For the gravity, it is found that the gravitational zero mode can be localized near zero. All the massive modes are continuous-spectrum wave functions and cannot be localized on the brane. For the scalar field, the zero mode is localized on the zero. For the vector field, if the coupling between vector and background spacetime is not introduced, the vector zero mode cannot be localized on the

brane, with the same case of RS brane. However, by introducing the coupling, the zero mode can be localized on the brane. For a large coupling coefficient, there exist vector resonant states, and the number of the resonances increases with the coupling coefficient. For the spin-1/2 fermion field, in order to localize the fermion zero mode, the coupling between the fermion and the background spacetime must be introduced. With a small coupling coefficient, only the left-chiral fermion zero mode is localized on the brane. However, with a large coupling coefficient, the left-chiral fermion zero mode is localized on the brane, and a finite number of resonant massive KK modes of the left- and right-chiral fermions are quasilocalized on the brane. And the number of resonances also increases with the coupling coefficient. Hence, the massless fermion is localized on the brane consists of just the left-chiral KK mode, and the massive fermions are quasilocalized on the brane consist of the left- and right-chiral fermion KK modes, represented the 4D Dirac massive fermions. The lifetime of the fermion KK resonant modes decreases with their masses.

ACKNOWLEDGMENTS

[1] N. Arkani-Hamed, S. Dimopoulos, and G. Dvali, The hierarchy problem and new dimensions at a millimeter, Phys. Lett. B **429**, 263 (1998).

[2] I. Antoniadis, N. Arkani-Hamed, S. Dimopoulos, and G. Dvali, New dimensions at a millimeter to a fermi and superstrings at a TeV, Phys. Lett. B **436**, 257 (1998).

[3] L. Randall and R. Sundrum, Large Mass Hierarchy from a Small Extra Dimension, Phys. Rev. Lett. **83**, 3370 (1999).

[4] M. Gogberashvili, Hierarchy problem in the shell-universe model, Int. J. Mod. Phys. D **11**, 1635 (2002).

[5] J. A. Cabrer, G. V. Gersdorff, and M. Quirós, Soft-wall stabilization, New J. Phys. **12**, 075012 (2010).

[6] J. M. Hoff da Silva and M. Dias, Five-dimensional $f(R)$ braneworld models, Phys. Rev. D **84**, 066011 (2011).

[7] K. Yang, Y. X. Liu, Y. Zhong, X. L. Du, and S. W. Wei, Gravity localization and mass hierarchy in scalar-tensor branes, Phys. Rev. D **86**, 127502 (2012).

[8] H. Guo, A. Herrera-Aguilar, Y. X. Liu, D. Malagón-Morejón, and R. R. Mora-Luna, Localization of bulk matter fields, the hierarchy problem and corrections to Coulomb's law on a pure de Sitter thick braneworld, Phys. Rev. D **87**, 095011 (2013).

[9] V. A. Rubakov and M. E. Shaposhnikov, Do we live inside a domain wall?, Phys. Lett. **125B**, 136 (1983).

[10] V. A. Rubakov and M. E. Shaposhnikov, Extra space-time dimensions: Towards a solution to the cosmological constant problem, Phys. Lett. **125B**, 139 (1983).

[11] S. Randjbar-Daemi and C. Wetterich, Kaluza-Klein solutions with non-compact internal spaces, Phys. Lett. **166B**, 65 (1986).

[12] E. J. Squires, Dimensional reduction caused by a cosmological constant, Phys. Lett. **167B**, 286 (1986).

[13] C. Csáki, J. Erlich, C. Grojean, and T. J. Hollowood, General properties of the self-tuning domain wall approach to the cosmological constant problem, Nucl. Phys. **B584**, 359 (2000).

[14] N. Arkani-Hamed, S. Dimopoulos, N. Kaloper, and R. Sundrum, A small cosmological constant from a large extra dimension, Phys. Lett. B **480**, 193 (2000).

[15] S. Kachru, M. Schulz, and E. Silverstein, Self-tuning flat domain walls in 5D gravity and string theory, Phys. Rev. D **62**, 045021 (2000).

[16] B. Bajc and G. Gabadadze, Localization of matter and cosmological constant on a brane in anti de Sitter space, Phys. Lett. B **474**, 282 (2000).

[17] J. E. Kim, B. Kyae, and H. M. Lee, Randall-Sundrum Model for Self-Tuning the Cosmological Constant, Phys. Rev. Lett. **86**, 4223 (2001).

[18] G. D. Starkman, D. Stojkovic, and M. Trodden, Homogeneity, Flatness, and "Large" Extra Dimensions, Phys. Rev. Lett. **87**, 231303 (2001).

[19] A. Kehagias and K. Tamvakis, A self-tuning solution of the cosmological constant problem, Mod. Phys. Lett. A **17**, 1767 (2002).

[20] A. Kehagias, A conical tear drop as a vacuum-energy drain for the solution of the cosmological constant problem, Phys. Lett. B **600**, 133 (2004).

[21] I. P. Neupane, De Sitter brane-world, localization of gravity, and the cosmological constant, Phys. Rev. D **83**, 086004 (2011).

[22] L. Randall and R. Sundrum, An Alternative to Compactification, Phys. Rev. Lett. **83**, 4690 (1999).

[23] F. Bonjour, C. Charmousis, and R. Gregory, Thick domain wall universes, Classical Quantum Gravity **16**, 2427 (1999).

[24] W. D. Goldberger and M. B. Wise, Modulus Stabilization with Bulk Fields, Phys. Rev. Lett. **83**, 4922 (1999).

[25] M. Gremm, Four-dimensional gravity on a thick domain wall, Phys. Lett. B **478**, 434 (2000).

[26] O. DeWolfe, D. Z. Freedman, S. S. Gubser, and A. Karch, Modeling the fifth dimension with scalars and gravity, Phys. Rev. D **62**, 046008 (2000).

[27] C. Csáki, J. Erlich, T. J. Hollowood, and Y. Shirman, Universal aspects of gravity localized on thick branes, Nucl. Phys. **B581**, 309 (2000).

[28] S. Ichinose, Some properties of domain wall solution in the Randall-Sundrum model, Classical Quantum Gravity **18**, 5239 (2001).

[29] S. Ichinose, A solution of the Randall-Sundrum model and the mass hierarchy problem, Classical Quantum Gravity **18**, 421 (2001).

[30] A. Campos, Critical Phenomena of Thick Branes in Warped Spacetimes, Phys. Rev. Lett. **88**, 141602 (2002).

[31] R. Gregory and A. Padilla, Nested braneworlds and strong brane gravity, Phys. Rev. D **65**, 084013 (2002).

[32] S. Kobayashi, K. Koyama, and J. Soda, Thick brane worlds and their stability, Phys. Rev. D **65**, 064014 (2002).

[33] K. A. Bronnikov and B. E. Meierovich, A general thick brane supported by a scalar field, Gravitation Cosmol. **9**, 313 (2003), arXiv:gr-qc/0402030.

[34] M. Eto and N. Sakai, Solvable models of domain walls in $\mathcal{N} = 1$ supergravity, Phys. Rev. D **68**, 125001 (2003).

[35] A. Melfo, N. Pantoja, and A. Skirzewski, Thick domain wall spacetimes with and without reflection symmetry, Phys. Rev. D **67**, 105003 (2003).

[36] D. Bazeia, C. Furtado, and A. R. Gomes, Brane structure from a scalar field in warped spacetime, J. Cosmol. Astropart. Phys. 02 (2004) 002.

[37] D. Bazeia, A. Gomes, and A. R. Gomes, Bloch brane, J. High Energy Phys. 05 (2004) 012.

[38] D. Bazeia, F. A. Brito, and L. Losano, Scalar fields, bent branes, and RG flow, J. High Energy Phys. 11 (2006) 064.

[39] V. I. Afonso, D. Bazeia, and L. Losano, First-order formalism for bent brane, Phys. Lett. B **634,** 526 (2006).

[40] V. Dzhunushaliev, Thick brane solution in the presence of two interacting scalar fields, Gravitation Cosmol. **13,** 302 (2007), arXiv:gr-qc/0603020.

[41] V. Afonso, D. Bazeia, R. Menezes, and A. Petrov, $f(R)$-branes, Phys. Lett. B **658,** 71 (2007).

[42] D. P. George and R. R. Volkas, Kink modes and effective four dimensional fermion and Higgs brane models, Phys. Rev. D **75,** 105007 (2007).

[43] V. Dzhunushaliev, V. Folomeev, D. Singleton, and S. Aguilar-Rudametkin, 6D thick branes from interacting scalar fields, Phys. Rev. D **77,** 044006 (2008).

[44] V. Dzhunushaliev, V. Folomeev, and M. Minamitsuji, Thick de Sitter brane solutions in higher dimensions, Phys. Rev. D **79,** 024001 (2009).

[45] D. Bazeia, A. Gomes, L. Losano, and R. Menezes, Braneworld models of scalar fields with generalized dynamics, Phys. Lett. B **671,** 402 (2009).

[46] D. Bazeia, A. R. Gomes, and L. Losano, Gravity localization on thick branes: A numerical approach, Int. J. Mod. Phys. A **24,** 1135 (2009).

[47] A. E. R. Chumbes and M. B. Hott, Nonpolynomial potentials with deformable topological structures, Phys. Rev. D **81,** 045008 (2010).

[48] Z. H. Zhao, Y. X. Liu, H. T. Li, and Y. Q. Wang, Effects of the variation of mass on fermion localization and resonances on thick branes, Phys. Rev. D **82,** 084030 (2010).

[49] Y. X. Liu, Y. Zhong, and K. Yang, Scalar-kinetic branes, Europhys. Lett. **90,** 51001 (2010).

[50] Y. X. Liu, Y. Zhong, Z. H. Zhao, and H. T. Li, Domain wall brane in squared curvature gravity, J. High Energy Phys. 06 (2011) 135.

[51] H. T. Li, Y. X. Liu, Z. H. Zhao, and H. Guo, Fermion resonances on a thick brane with a piecewise warp factor, Phys. Rev. D **83,** 045006 (2011).

[52] H. Guo, Y. X. Liu, Z. H. Zhao, and F. W. Chen, Thick branes with a nonminimally coupled bulk-scalar field, Phys. Rev. D **85,** 124033 (2012).

[53] H. Guo, Y. X. Liu, S. W. Wei, and C. E. Fu, Gravity localization and effective Newtonian potential for Bent thick branes, Europhys. Lett. **97,** 60003 (2012).

[54] D. Bazeia, F. A. Brito, and F. G. Costa, Braneworld solutions from scalar field in bimetric theory, Phys. Rev. D **87,** 065007 (2013).

[55] A. de Souza Dutra, G. P. de Brito, and J. M. H. da Silva, Method for obtaining thick brane models, Phys. Rev. D **91,** 086016 (2014).

[56] G. Germán, A. Herrera-Aguilar, D. Malagón-Morejón, I. Quiros, and R. da Rocha, Study of field fluctuations and their localization in a thick braneworld generated by gravity nonminimally coupled to a scalar field with the Gauss-Bonnet term, Phys. Rev. D **89,** 026004 (2014).

[57] D. Bazeia, A. S. Lobáo, Jr, R. Menezes, A. Y. Petrov, and A. J. da Silva, Braneworld solutions for $F(R)$ models with non-constant curvature, Phys. Lett. B **729,** 127 (2014).

[58] D. Bazeia, A. S. Lobáo, Jr, and R. Menezes, Thick brane models in generalized theories of gravity, Phys. Lett. B **743,** 98 (2015).

[59] D. Bazeia, A. S. Lobáo, Jr, L. Losano, R. Menezes, and G. J. Olmo, Braneworld solutions for modified theories of gravity with nonconstant curvature, Phys. Rev. D **91,** 124006 (2015).

[60] D. Bazeia, L. Losano, R. Menezes, G. J. Olmo, and D. Rubiera-Garcia, Thick brane in $f(R)$ gravity with Palatini dynamics, Eur. Phys. J. C **75,** 569 (2015).

[61] B. Guo, Y. X. Liu, and K. Yang, Brane worlds in gravity with auxiliary fields, Eur. Phys. J. C **75,** 63 (2015).

[62] L. Visinelli, N. Bolis, and S. Vagnozzi, Brane-world extra dimensions in light of GW170817, Phys. Rev. D **97,** 064039 (2018).

[63] S. SenGupta, Aspects of warped braneworld models, arXiv:0812.1092.

[64] V. Dzhunushaliev, V. Folomeev, and M. Minamitsuji, Thick brane solutions, Rep. Prog. Phys. **73,** 066901 (2010).

[65] M. Shifman, Large extra dimensions: Becoming acquainted with an alternative paradigm, Int. J. Mod. Phys. A **25,** 199 (2010).

[66] T. G. Rizzo, Introduction to extra dimensions, AIP Conf. Proc. **1256,** 27 (2010).

[67] R. Maartens and K. Koyama, Brane-world gravity, Living Rev. Relativity **13,** 5 (2010).

[68] O. Arias, R. Cardenas, and I. Quiros, Thick brane worlds arising from pure geometry, Nucl. Phys. **B643,** 187 (2002).

[69] N. Barbosa-Cendejas and A. Herrera-Aguilar, 4D gravity localized in non $\mathbb{Z}_2$ -symmetric thick branes, J. High Energy Phys. 10 (2005) 101.

[70] N. Barbosa-Cendejas and A. Herrera-Aguilar, Localization of 4D gravity on pure geometrical thick branes, Phys. Rev. D **73,** 084022 (2006).

[71] N. Barbosa-Cendejas, A. Herrera-Aguilar, M. A. R. Santos, and C. Schubert, Mass gap for gravity localized on Weyl thick branes, Phys. Rev. D **77,** 126013 (2008).

[72] Y. X. Liu, K. Yang, and Y. Zhong, De Sitter thick brane solution in Weyl geometry, J. High Energy Phys. 10 (2010) 069.

[73] V. Dzhunushaliev, V. Folomeev, B. Kleihaus, and J. Kunz, Some thick brane solutions in $f(R)$-gravity, J. High Energy Phys. 04 (2010) 130.

[74] H. Liu, H. Lü, and Z. L. Wang, $f(R)$ gravities, killing spinor equations, "BPS" domain walls and cosmology, J. High Energy Phys. 02 (2012) 083.

[75] J. Yang, Y. L. Li, Y. Zhong, and Y. Li, Thick brane split caused by spacetime torsion, Phys. Rev. D **85,** 084033 (2012).

[76] N. Barbosa-Cendejas, A. Herrera-Aguilar, K. Kanakoglou, U. Nucamendi, and I. Quiros, Mass hierarchy, mass gap and corrections to Newton's law on thick branes with Poincaré symmetry, Gen. Relativ. Gravit. **46,** 1631 (2014).

[77] Y. Zhong and Y. X. Liu, Pure geometric thick $f(R)$-branes: Stability and localization of gravity, Eur. Phys. J. C **76,** 321 (2016).

[78] Y. X. Liu, X. H. Zhang, L. D. Zhang, and Y. S. Duan, Localization of matters on pure geometrical thick branes, J. High Energy Phys. 02 (2008) 067.

[79] Y. X. Liu, L. D. Zhang, L. J. Zhang, and Y. S. Duan, Fermions on thick branes in the background of sine-Gordon kinks, Phys. Rev. D **78,** 065025 (2008).

[80] Y. X. Liu, L. D. Zhang, S. W. Wei, and Y. S. Duan, Localization and mass spectrum of matters on Weyl thick branes, J. High Energy Phys. 08 (2008) 041.

[81] Y. X. Liu, H. Guo, C. E. Fu, and H. T. Li, Localization of gravity and bulk matters on a thick anti-de Sitter brane, Phys. Rev. D **84,** 044033 (2011).

[82] Z. H. Zhao, Q. Y. Xie, and Y. Zhong, New localization method of $U(1)$ gauge vector field on flat branes in (asymptotic) AdS$_5$ spacetime, Classical Quantum Gravity **32,** 035020 (2015).

[83] Z. H. Zhao and Q. Y. Xie, Localization of $U(1)$ gauge vector field on flat branes with five-dimension (asymptotic) AdS$_5$ spacetime, J. High Energy Phys. 05 (2018) 072.

[84] S. Randjbar-Daemi and M. Shaposhnikov, Fermion zero-modes on brane-worlds, Phys. Lett. B **492,** 361 (2000).

[85] S. L. Dubovsky, V. A. Rubakov, and P. G. Tinyakov, Brane world: Disappearing massive matter, Phys. Rev. D **62,** 105011 (2000).

[86] T. Gherghetta and M. Shaposhnikov, Localizing Gravity on a Stringlike Defect in Six Dimensions, Phys. Rev. Lett. **85,** 240 (2000).

[87] Y. Grossman and M. Neubert, Neutrino masses and mixings in non-factorizable geometry, Phys. Lett. B **474,** 361 (2000).

[88] A. Kehagias and K. Tamvakis, Localized gravitons, gauge bosons and chiral fermions in smooth spaces generated by a bounce, Phys. Lett. B **504,** 38 (2001).

[89] I. Oda, Localization of matters on a string-like defect, Phys. Lett. B **496,** 113 (2000).

[90] I. P. Neupane, Consistency of higher derivative gravity in the brane background, J. High Energy Phys. 09 (2000) 040.

[91] I. P. Neupane, Completely localized gravity with higher curvature terms, Classical Quantum Gravity **19,** 5507 (2002).

[92] S. Ichinose, Fermions in Kaluza-Klein and Randall-Sundrum theories, Phys. Rev. D **66,** 104015 (2002).

[93] C. Ringeval, P. Peter, and J. P. Uzan, Localization of massive fermions on the brane, Phys. Rev. D **65,** 044016 (2002).

[94] A. A. Andrianov, V. A. Andrianov, P. Giacconi, and R. Soldati, Domain wall generation by fermion self-interaction and light particles, J. High Energy Phys. 07 (2003) 063.

[95] A. A. Andrianov, V. A. Andrianov, P. Giacconi, and R. Soldati, Brane world generation by matter and gravity, J. High Energy Phys. 07 (2005) 003.

[96] R. Koley and S. Kar, A novel braneworld model with a bulk scalar field, Phys. Lett. B **623,** 244 (2005).

[97] R. Koley and S. Kar, Scalar kinks and fermion localization in warped spacetimes, Classical Quantum Gravity **22,** 753 (2005).

[98] Y. Q. Wang, T. Y. Si, Y. X. Liu, and Y. S. Duan, Fermionic zero modes in self-dual vortex background, Mod. Phys. Lett. A **20,** 3045 (2005).

[99] A. Melfo, N. Pantoja, and J. D. Tempo, Fermion localization on thick branes, Phys. Rev. D **73,** 044033 (2006).

[100] A. Salvio and M. Shaposhnikov, Chiral asymmetry from a 5D Higgs mechanism, J. High Energy Phys. 11 (2007) 037.

[101] T. R. Slatyer and R. R. Volkas, Cosmology and fermion confinement in a scalar-field-generated domain wall brane in five dimensions, J. High Energy Phys. 04 (2007) 062.

[102] Y. X. Liu, L. Zhao, and Y. S. Duan, Localization of fermions on a string-like defect, J. High Energy Phys. 04 (2007) 097.

[103] Y. X. Liu, L. Zhao, X. H. Zhang, and Y. S. Duan, Fermions in self-dual vortex background on a string-like defect, Nucl. Phys. **B785,** 234 (2007).

[104] Y. Brihaye and T. Delsate, Remarks on bell-shaped lumps: Stability and fermionic modes, Phys. Rev. D **78,** 025014 (2008).

[105] L. Zhao, Y. X. Liu, and Y. S. Duan, Fermions in gravity and gauge backgrounds on a brane world, Mod. Phys. Lett. A **23,** 1129 (2008).

[106] M. O. Tahim, W. T. Cruz, and C. A. S. Almeida, Tensor gauge field localization in branes, Phys. Rev. D **79,** 085022 (2009).

[107] A. Flachi and M. Minamitsuji, Field localization on a brane intersection in anti-de Sitter spacetime, Phys. Rev. D **79,** 104021 (2009).

[108] Y. Kodama, K. Kokubu, and N. Sawado, Localization of massive fermions on the baby-Skyrmion branes in 6 dimensions, Phys. Rev. D **79,** 065024 (2009).

[109] Y. X. Liu, J. Yang, Z. H. Zhao, C. E. Fu, and Y. S. Duan, Fermion localization and resonances on a de Sitter thick brane, Phys. Rev. D **80,** 065019 (2009).

[110] Y. X. Liu, C. E. Fu, L. Zhao, and Y. S. Duan, Localization and mass spectra of fermions on symmetric and asymmetric thick branes, Phys. Rev. D **80,** 065020 (2009).

[111] Y. X. Liu, Z. H. Zhao, S. W. Wei, and Y. S. Duan, Bulk matters on symmetric and asymmetric de Sitter thick branes, J. Cosmol. Astropart. Phys. 02 (2009) 003.

[112] C. A. S. Almeida, R. Casana, M. M. Ferreira, and A. R. Gomes, Fermion localization and resonances on two-field thick branes, Phys. Rev. D **79,** 125022 (2009).

[113] R. Koley, J. Mitra, and S. SenGupta, Fermion localization in a generalized Randall-Sundrum model, Phys. Rev. D **79,** 041902 (2009).

[114] L. B. Castro, Fermion localization on two-field thick branes, Phys. Rev. D **83,** 045002 (2011).

[115] A. E. R. Chumbes, A. E. O. Vasquez, and M. B. Hott, Fermion localization on a split brane, Phys. Rev. D **83,** 105010 (2011).

[116] W. T. Cruz, A. R. Gomes, and C. A. S. Almeida, Fermions on deformed thick branes, Eur. Phys. J. C **71,** 1790 (2011).

[117] C. E. Fu, Y. X. Liu, and H. Guo, Bulk matter fields on two-field thick branes, Phys. Rev. D **84,** 044036 (2011).

[118] O. Castillo-Felisola and I. Schmidt, Localization of fermions in different domain wall models, Phys. Rev. D **86,** 024014 (2012).

[119] T. Delsate and N. Sawado, Localizing modes of massive fermions and a $U(1)$ gauge field in the inflating baby-Skyrmion branes, Phys. Rev. D **85,** 065025 (2012).

[120] A. A. Andrianov, V. A. Andrianov, and O. O. Novikov, *CP* Violation in the models of fermion localization on a domain wall (brane), Theor. Math. Phys. **175**, 735 (2013).

[121] V. K. Oikonomou, Localized fermions on domain walls and extended supersymmetric quantum mechanics, Classical Quantum Gravity **31**, 025018 (2013).

[122] M. Gogberashvili and P. Midodashvili, Fermions in the 5D gravity-scalar standing wave braneworld, Int. J. Mod. Phys. A **29**, 1450141 (2014).

[123] L. J. S. Sousa, C. A. S. Silva, D. M. Dantas, and C. A. S. Almeida, Vector and fermion fields on a bouncing brane with a decreasing warp factor in a string-like defect, Phys. Lett. B **731**, 64 (2014).

[124] Y. X. Liu, Z. G. Xu, F. W. Chen, and S. W. Wei, New localization mechanism of fermions on braneworlds, Phys. Rev. D **89**, 086001 (2014).

[125] N. Barbosa-Cendejas, D. Malagón-Morejón, and R. R. Mora-Luna, Universal spin-1/2 fermion field localization on a 5D braneworld, Gen. Relativ. Gravit. **47**, 77 (2015).

[126] H. Guo, Q. Y. Xie, and C. E. Fu, Localization and quasilocalization of a spin-1/2 fermion field on a two-field thick braneworld, Phys. Rev. D **92**, 106007 (2015).

[127] I. C. Jardim, G. Alencar, R. R. Landim, and R. N. C. Filho, Solutions to the problem of Elko spinor localization in brane models, Phys. Rev. D **91**, 085008 (2015).

[128] R. Cartas-Fuentevilla, A. Escalante, G. Germán, A. Herrera-Aguilar, and R. R. Mora-Luna, Coulomb's law corrections and fermion field localization in a tachyonic de Sitter thick braneworld, J. Cosmol. Astropart. Phys. 05 (2016) 026.

[129] Y. Y. Li, Y. P. Zhang, W. D. Guo, and Y. X. Liu, Fermion localization mechanism with derivative geometrical coupling on branes, Phys. Rev. D **92**, 115003 (2017).

[130] V. F. Mukhanov, L. A. Kofman, and D. Y. Pogosyan, Cosmological perturbations in the inflationary universe, Phys. Lett. B **193**, 427 (1987).

[131] J. D. Barrow and S. Cotsakis, Inflation and the conformal structure of higher-order gravity theories, Phys. Lett. B **214**, 515 (1988).

[132] G. Cognola, E. Elizalde, S. Nojiri, S. D. Odintsov, L. Sebastiani, and S. Zerbini, Class of viable modified $f(R)$ gravities describing inflation and the onset of accelerated expansion, Phys. Rev. D **77**, 046009 (2008).

[133] A. D. Felice and S. Tsujikawa, $f(R)$ theories, Living Rev. Relativity **13**, 3 (2010).

[134] T. P. Sotiriou and V. Faraoni, $f(R)$ theories of gravity, Rev. Mod. Phys. **82**, 451 (2010).

[135] S. Nojiri and S. D. Odintsov, Unified cosmic history in modified gravity: From $F(R)$ theory to Lorentz non-invariant models, Phys. Rep. **505**, 59 (2011).

[136] N. Dimakis, A. Giacomini, and A. Paliathanasis, Black branes in four-dimensional conformal equivalent theories, Eur. Phys. J. C **78**, 751 (2018).

[137] N. Dimakis, A. Giacomini, and A. Paliathanasis, (Compactified) black branes in four dimensional $f(R)$-gravity, Phys. Lett. B **777**, 059 (2018).

[138] R. Myrzakulov, L. Sebastiani, and S. Vagnozzi, Inflation in $f(R, \phi)$-theories and mimetic gravity scenario, Eur. Phys. J. C **75**, 444 (2015).

[139] V. Dzhunushaliev, V. Folomeev, G. Nurtaeva, and S. D. Odintsov, Thick branes in higher-dimensional $f(R)$ gravity, Int. J. Geom. Methods Mod. Phys. **17**, 2050036 (2020).

[140] M. Parry, S. Pichler, and D. Deeg, Higher-derivative gravity in brane world models, J. Cosmol. Astropart. Phys. 04 (2005) 014.

[141] N. Deruelle, M. Sasaki, and Y. Sendouda, Junction conditions in $f(R)$ theories of gravity, Prog. Theor. Phys. **119**, 237 (2008).

[142] A. Balcerzak and M. P. Dabrowski, Generalized Israel junction conditions for a fourth-order brane world, Phys. Rev. D **77**, 023524 (2008).

[143] A. Balcerzak and M. P. Dabrowski, Gibbons-Hawking boundary terms and junction conditions for higher-order brane gravity models, J. Cosmol. Astropart. Phys. 01 (2009) 018.

[144] Y. Zhong, Y. X. Liu, and K. Yang, Tensor perturbations of $f(R)$-branes, Phys. Lett. B **699**, 398 (2011).

[145] T. R. P. Carames, M. E. X. Guimaraes, and J. M. H. da Silva, Effective gravitational equations for $f(R)$ brane-world models, Phys. Rev. D **87**, 106011 (2013).

[146] D. Bazeia, R. Menezes, A. Y. Petrov, and A. J. da Silva, On the many-field $f(R)$ brane, Phys. Lett. B **726**, 523 (2013).

[147] Z. G. Xu, Y. Zhong, H. Yu, and Y. X. Liu, The structure of $f(R)$-brane model, Eur. Phys. J. C **75**, 368 (2015).

[148] B. M. Gu, B. Guo, H. Yu, and Y. X. Liu, Tensor perturbations of Palatini $f(\mathbf{R})$ branes, Phys. Rev. D **92**, 02401 (2015).

[149] H. Yu, Y. Zhong, B. M. Gu, and Y. X. Liu, Gravitational resonances on $f(R)$-brane, Eur. Phys. J. C **76**, 195 (2016).

[150] Z. Q. Cui, Y. X. Liu, B. M. Gu, and L. Zhao, Linear stability of $f(R, \phi, X)$ thick branes: Tensor perturbations, J. High Energy Phys. 11 (2018) 083.

[151] A. Herrera-Aguilar, D. Malagón-Morejón, and R. Rigel Mora-Luna, Localization of gravity on a de Sitter thick braneworld without scalar fields, J. High Energy Phys. 11 (2010) 015.

[152] Q. Y. Xie, J. Yang, and L. Zhao, Resonance mass spectra of gravity and fermion on Bloch branes, Phys. Rev. D **88**, 105014 (2013).